ELSEVIER

Coordination Chemistry Reviews 225 (2002) 91–121

COORDINATION CHEMISTRY REVIEWS

www.elsevier.com/locate/ccr

Classification of coordination polygons and polyhedra according to their mode of self-assembly. 2. Review of the literature

Gerhard F. Swiegers *, Tshepo J. Malefetse [1]

Division of Molecular Science, Commonwealth Scientific and Industrial Research Organisation (CSIRO), Bag 10, Clayton South, Victoria 3169, Australia

Received 29 March 2001; accepted 6 July 2001

Contents

Abbreviations: Oac$^-$, acetate; acac, acetylacetonate; binap, 2,2′-bis(diphenylphosphino)-1,1′-binaphthyl; dppp, 1,3-bis(diphenylphosphino)propane; cyclen, 1,4,7,10-tetraazacyclododecane; cod, cyclooctadiene; diop, 2,3-*o*-isopropylidene-2,3-dihydroxy-1,4-bis(diphenylphosphino)butane; en, 1,2-ethylenediamine; triphos, 1,1,1-tris(diphenylphosphinomethane)ethane.

* Corresponding author. Tel.: +61-3-9545-2528; fax: +61-3-9545-2589.

E-mail address: g.swiegers@molsci.csiro.au (G.F. Swiegers).

[1] Visiting Fellow. Home address: Center for Applied Chemistry and Chemical Technology, Department of Chemistry, University of the Witwatersrand, Private Bag 3, Wits 2050, South Africa.

0010-8545/02/$ - see front matter Published by Elsevier Science B.V.
PII: S0010-8545(01)00407-6

Abstract

Numerous molecular polygons and polyhedra, formed by metal-mediated self-assembly, have been described in the chemical literature in recent years. This work reviews such compounds in terms of the recently described 'assembly descriptor' classification which groups them according to similarity in the stoichiometry and building block topicity of their self-assembly. Relationships between different ensemble types and the application of the new system to the controlled, rational preparation of novel assemblies is emphasised. Published by Elsevier Science B.V.

Keywords: Metallocycles; Self-assembly; Supramolecular chemistry; Metallocycles

1. Introduction

The study of self-assembling systems in coordination chemistry has delivered a wide variety of discrete molecular architectures in recent years, including twisted structures (e.g. helicates), latticed structures (e.g. grids, racks, ladders), filamentous structures (e.g. rods, metallodendrimers), and interlaced structures (e.g. rotaxanes, catenanes, knots) [1,2]. Perhaps the most interesting architectures, however, are to be found in the closed, geometrically-shaped, 2-D and 3-D structures known as metallocyclic polygons and polyhedra [2]. These materials have been variously termed molecular triangles, squares, hexagons, cubes, and so forth, because of their resemblance to the corresponding geometric form. Such molecules typically contain central cavities, allowing them to act as artificial molecular-scale containers or receptors. In doing so, they may exhibit unusual electrochemical, magnetochemical, photoluminescent, catalytic, or synthetic chemical effects.[2]

The classification of molecular polygons and polyhedra into a useful system of understanding has proved particularly problematic because of the large diversity of architectural forms available. However, we have recently demonstrated that the commonality of their self-assembly provides a helpful means of categorising such compounds without losing sight of each one's distinctive overall shape [3]. The 'assembly descriptor' nomenclature abbreviates—uniquely—the self-assembly process using a formula-like notation to indicate the type, stoichiometry, and topicity of the building blocks involved in the formation of a particular compound [3]. This classification allows a ready comparison with similarly assembled compounds even if they have very different overall shapes. It also: (i) facilitates the systematic identification of acceptor–donor combinations which are suitable for the formation of a particular product architecture, (ii) reveals useful commonalities between compounds of different structure and mode of assembly (e.g. the use of building blocks of identical topicity), (iii) aids in the conceptual development and practical preparation of novel architectures, and (iv) provides a means to identify systematically systems capable of being switched back-and-forth between architectures [3].

This work aims to provide a reference source which describes known metallocyclic polygons and polyhedra in terms of their assembly descriptor notation. Compounds have been grouped according to their descrip-

---

[2] Examples of the possible applications of geometric metallocyclic polygons and polyhedra are discussed in Refs. [1,2a].

tors in order to facilitate a comparison with newly conceived or prepared complexes. The relationships between different ensemble types and the application of this system to the controlled, rational preparation of novel assemblies have been particularly noted. The review covers the period to September 2000.

2. The assembly descriptor notation

The assembly descriptor notation employed in this work is a modification of that originally described by Stang [4]. The modification is necessary to ensure the uniqueness of each descriptor.

Each building block in an assembly is designated as either linear ('L'; directing angle 180°) or angular ('A'; directing angle < 180°). The topicity of each building block, defined as the number of links it can form with a complementary building block, is indicated after its designation using a superscript which contains 'a's (acceptor) and/or 'd's (donor) to indicate the types of binding sites present. Identical binding sites on the same building block are combined into a single 'a' or 'd' with a preceding numeral to indicate the number of these sites. Non-identical sites are designated separately. Thus, a tritopic angular building block containing three identical acceptor binding sites, such as that depicted in Fig. 1, has the notation A^{3a}. The linear unit illustrated in Fig. 1 contains two non-identical donor binding sites and is therefore symbolised L^{1d1d}.

The descriptor of an assembly is composed of the notation for each building block, subscripted to indicate its stoichiometry. Thus, an assembly consisting of two of the A^{3a} units described above and three of the L^{1d1d} units will have the descriptor $A_2^{3a}L_3^{1d1d}$ (Fig. 1). The order in which the building blocks are listed in an assembly descriptor is as follows: units incorporating only acceptor binding sites are listed first followed by hybrid building blocks which contain both acceptor and donor sites. Units incorporating only donor sites are listed last. Where several donor or acceptor building blocks are present, these are listed in order of *decreasing topicity*.

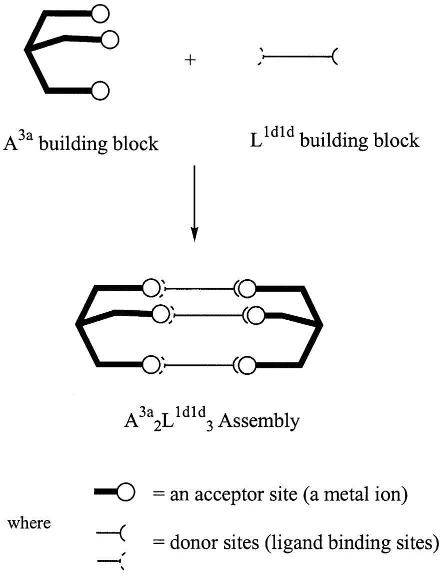

Fig. 1. Schematic illustrating the formation of a hypothetical $A_2^{3a}L_3^{d1d}$ molecular box by metal-mediated self-assembly.

These descriptors not only succinctly describe the self-assembly process, but also give information regarding the number of links formed between the building blocks and the presence or absence of free, unbound linkage sites. To form species which have the greatest enthalpic stability, the number of links formed by the acceptor and donor sites must be equal and the maximum number possible. It should also be noted that this notation does not necessarily describe the number of bonds formed in the self-assembly. For example, the link between a bidentate chelate (a donor-based binding site) and a ditopic metal ion (an acceptor-based binding site) is considered a single link despite the fact that it involves two coordinate bonds. This distinction permits a description of the widest possible variety of species, including ones formed or partially formed by non-coordinate, non-covalent interactions.

3. Classification of known coordinate polygons and polyhedra according to their mode of self-assembly

In this section, previously reported molecular polygons and polyhedra are grouped in terms of their assembly descriptor notation rather than their overall shape. To best illustrate the relationships between the different self-assembled structures, examples having identical descriptors have been grouped together. Each of these collections have then been further sorted according to the number of acceptor-based building blocks present. It should be noted that the latter categorisation has been employed purely to facilitate a recognition of the commonalities present; metal ion-based units provide the best reference for coordination chemists. Other groupings may be more suitable for other linkage types or to illustrate other relationships.

3.1. Self-cyclised assemblies

All self-cyclised assemblies to date have produced 2-D polygons, although many of these are puckered or not entirely planar in some way. However, there is no reason that 3-D polyhedra should not be obtained using hybrid building blocks.

3.1.1. A_2^{1a1d} assemblies

A_2^{1a1d} assemblies are the least complicated of self-assembled coordination compounds and possibly also one

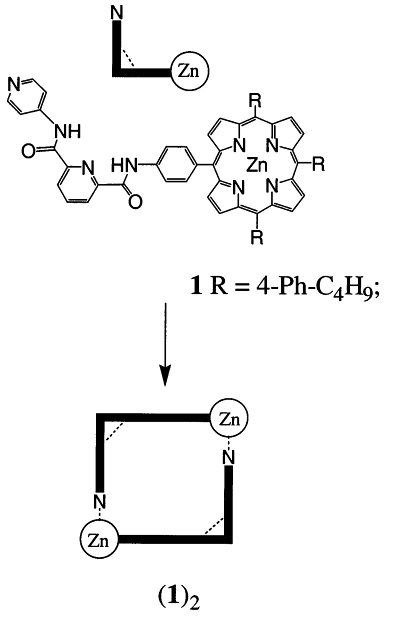

1 R = 4-Ph-C_4H_9;

(1)$_2$

Scheme 1.

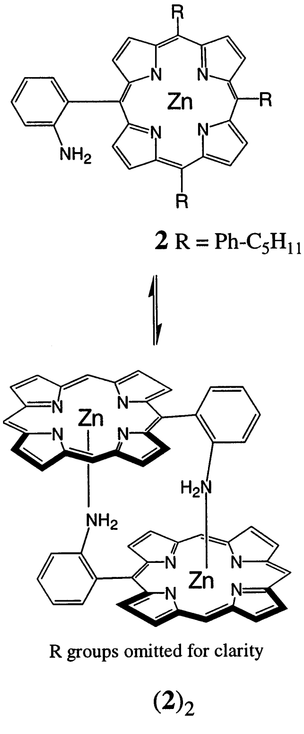

2 R = Ph-C_5H_{11}

R groups omitted for clarity

(2)$_2$

Scheme 2.

of the most difficult to prepare. For an A_2^{1a1d} ensemble to be cyclic, each building block must be able to enclose an angle of 360° between its donor and acceptor binding sites. To the best of our knowledge, only two examples of such ensembles are known; both involve substituted porphyrins and both result in 2-D molecular squares.

The zincated porphyrin **1** spontaneously forms the A_2^{1a1d} square (**1**)$_2$ by intermolecular Zn–N coordination at 10^{-2}–10^{-7} M in chloroform at room temperature (Scheme 1) [5]. This dimer is strongly stabilised by intramolecular hydrogen bonding within the arms of the substituent chain. The effect of the hydrogen bonding is to reduce the angle subtended by the linkers from the 120° expected for *meta*-substituted pyridyls to approximately 96°. As a consequence, the squares are somewhat tetragonally distorted.

An aniline substituent on a porphyrin skeleton is a significantly more rigid linker than the side-chains of **1**. However, Hunter and co-workers [6] have demonstrated that when *o*- or *m*-aniline substituents are used, zinc aminoporphyrins like **2** form Zn–N bound dimers in solution (Scheme 2). In these cases, free rotation about the aniline–porphyrin bond allows the formation of a coordinate bond roughly orthogonal to the plane of the porphyrin, with A_2^{1a1d} squares of type (**2**)$_2$ generated at particular solution concentrations. When *p*-aniline is used as a substituent, the amine *N*-atom is unable to coordinate, so that coordination oligomers and polymers result [6].

3.1.2. A_3^{1a1d} assemblies

If symmetrical, planar ligands are used with large and sterically unhindered metal-ions, A_3^{1a1d} assemblies

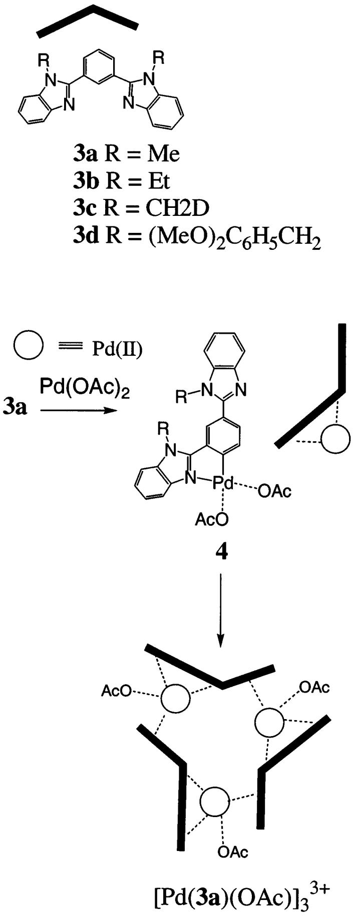

3a R = Me
3b R = Et
3c R = CH2D
3d R = $(MeO)_2C_6H_5CH_2$

$[Pd(\mathbf{3a})(OAc)]_3^{3+}$

Scheme 3.

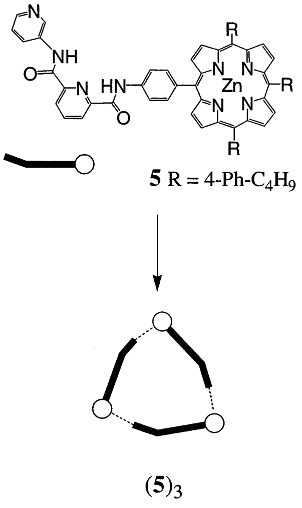

Scheme 4.

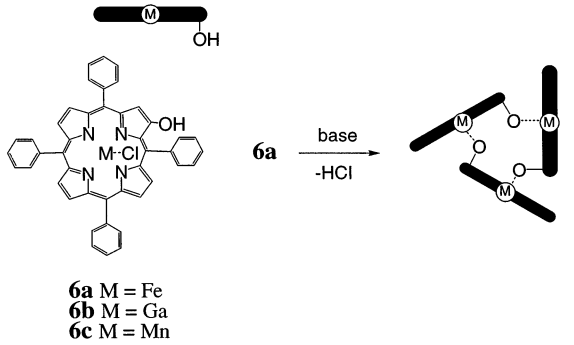

Scheme 5.

can be expected to produce 2-D molecular triangles. However, ideal ligands and metals of this type are rarely available, so that A_3^{1a1d} assemblies often exhibit a puckered "tricorn" shape.

The tricorn complex $[Pd_3(\mathbf{3a})_3(OAc)_3]^{3+}$ depicted in Scheme 3 is an example of an A_3^{1a1d} assembly ($OAc^- =$ acetate) [7]. It forms spontaneously when **3a** is treated with $Pd(OAc)_2$. The initial step in this reaction involves the irreversible formation of the cylometallated Pd–bis(-benzimidazol)benzene species **4**, which then undergoes replacement of one acetate with a *N*-donor on a neighbouring complex [7b]. The cavity in the tricorn is chiral, so that two mirror image enantiomers are formed; the cavity is occupied by an acetonitrile molecule in the solid state.

The self-cyclisation of metallated porphyrins containing pendant pyridine (**5**) [8] or hydroxy groups (**6**) [9] may also generate A_3^{1a1d} assemblies (Schemes 4 and 5) [8,9a]. The former complex is of particular interest since **5** differs from **1** only in the presence of a terminal 3-pyridyl, rather than a 4-pyridyl binding site. The effect of this apparently minor alteration is to stabilise selectively the A_3^{1a1d} assembly $(\mathbf{5})_3$ over the corresponding A_2^{1a1d} assembly seen in the case of **1**. The assemblies $(\mathbf{6})_3$ were obtained only in the presence of base [9a]. As no competing oligomeric products were observed, it is possible that a "self-correcting" thermodynamic equilibrium involving H–O–Fe coordination occurred prior to formation of the Fe–O–porphyrin bonds.

Treatment, at high pH, of the Co^{III} complex **7**, which contains a purine-based ligand, resulted in the partial formation (20%) of the A_3^{1a1d} C_1-symmetric triangle **8b** (Fig. 2) [10]. Despite the theoretical possibility of forming **8a** and **8c–e**, the only other product obtained was **8f**; a thermodynamic equilibrium or a strongly channelled, kinetically irreversible process must be responsible. To overcome the kinetic inertness of Co^{III}, the self-assembly process was initiated by the addition of NaOH to deprotonate the purine amines. The resulting triangle was kinetically stable, allowing it to be optically resolved into its mirror image isomers by elution on a Sephadex column with a chiral eluant.

3.1.3. A_4^{1a1d} assemblies

Several A_4^{1a1d} assemblies are known; all have 2-D square structures. Zincated porphyrins substituted with pyridine [5,8,11] groups have been employed in the self-assembly of several such structures. For example, Scheme 6 illustrates the formation of the A_4^{1a1d} square $(\mathbf{9})_4$, which is secured by intermolecular Zn–N(pyridyl) coordination bonds [8]. Porphyrins substituted with sulfoxide groups have been similarly employed; Fig. 3 depicts one such square [12]. Ruthenated A_4^{1a1d} square assemblies of this type are also known [13].

Other A_4^{1a1d} assemblies involve Ti–N coordinate bonds (e.g. $[(Cp_2Ti)_4(\mathbf{10})_4]^{4+}$ in Scheme 7) [14] and Cu^{II} bonds with pyridyl–azine–methylimidazol type ligands [15].

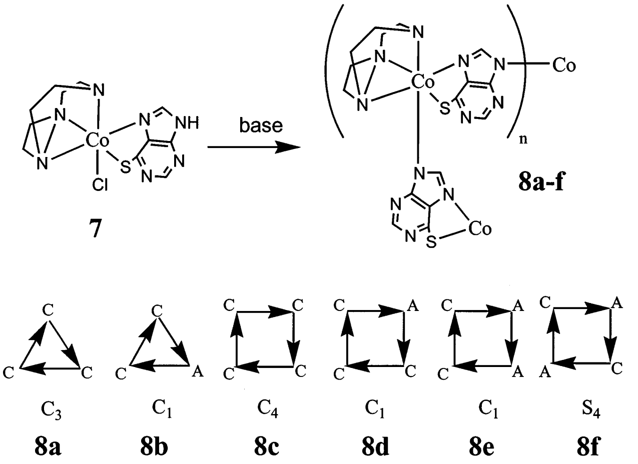

Fig. 2. Schematic depicting the formation of, and possible geometric isomers of the cyclic triangles and squares of purine-6-thione with 1,4,7-triazacyclonane–Co(III). The arrows depicted in **8a–f** illustrate the directionality of the linking purines. The characters at the corners of each structure, C (clockwise) and A (anti-clockwise), denote the chirality of each Co(III) unit.

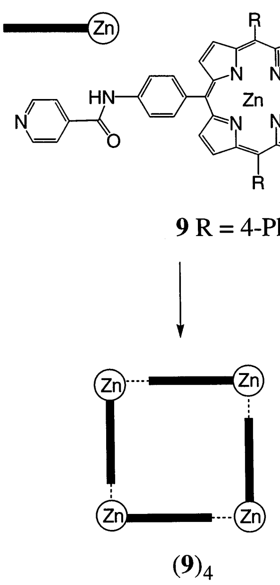

Scheme 6.

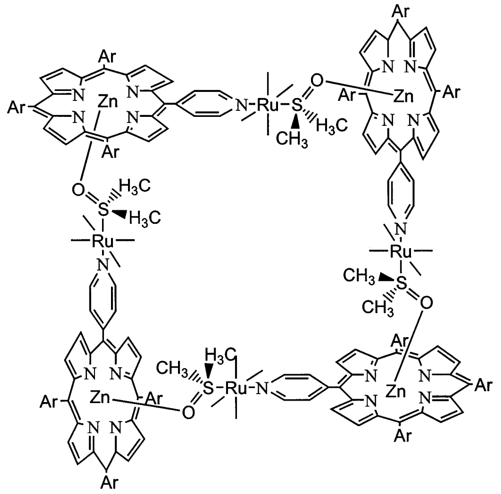

Fig. 3. Schematic depiction of a molecular square secured by SO–Zn bonds.

3.1.4. A_6^{1a1d} assemblies

A_6^{1a1d} assemblies generally form molecular hexagons. When the aquated monomeric Cu^{II} complex $[H(\mathbf{11})(H_2O)]^{2+}$ was deprotonated, it spontaneously self-cyclised to form the hexagonal A_6^{1a1d} compound $(\mathbf{11})_6^{6+}$ (Scheme 8) [15]. While square planar Cu^{II} normally binds at an angle of 90°, the presence of the bulky 2-phenyl substituent in **11** made a square structure impossible. Instead a distorted stereochemistry formed about each Cu^{II} ion, resulting in N–Cu–N binding angles of between 94.7 and 173.1°. The complex therefore displayed a puckered hexagonal structure. Replacement of the 2-phenyl substituent with a less-bulky methyl substituent resulted in the formation of the corresponding A_4^{1a1d} square. The 2-H analogue of **11** also delivered a A_6^{1a1d} hexagon [15b].

3.2. Multiple-component assemblies

3.2.1. A_1^{na} and L_1^{na} assemblies

Assemblies involving a single acceptor unit are somewhat rare because few ligands can produce a closed 2-D structure when combined with only one acceptor building block. A few examples are known however. One involves the reaction of the 4-pyridyl substituted porphyrin **12** with compound **13**, which contains two, zincated porphyrins tethered to each other by a terephthaloyl diamine linker (Scheme 9). The resulting $A_1^{2a}A_1^{2d}$ assembly, [(**12**)(**13**)], is secured by Zn–N coordinate bonds and is highly stable [11]. The only other known ensemble of this type employs **12** and an analogue of **13** containing a naphthalenediimide linker [11].

The need in this class of ensemble for a ditopic donor unit which encloses an angle of 360° upon binding is

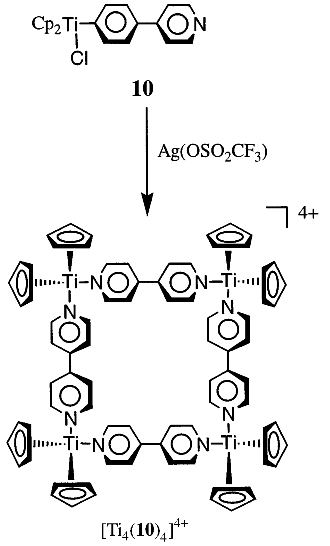

Scheme 7.

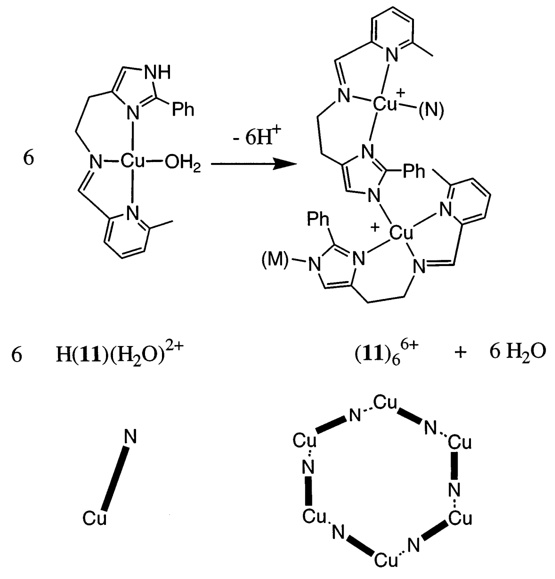

Scheme 8.

reminiscent of a similar requirement in $L_2^{2a}A_2^{2d}$ assemblies (vide infra Section 3.2.2.2). In those cases however, the metal ion acceptor sites are not incorporated into one of the building blocks as they are in **13**.

The somewhat flexible $A_1^{3a}A_1^{3d}$ molecular cage [(**14**)(**15**)] has also been recently reported (Scheme 10) [16]. This compound is formed when a tripodal tris(aminoethyl)amine ligand **15**, which is functionalised on its arms with pyridine (or methylimidazole), coordinates apically to the trisporphyrin derivative **14** (via Zn–N bonds).

To the best of our knowledge, examples of $A_1^{2a}L_1^{2d}$ or $L_1^{2a}A_1^{2d}$ and their tri- and multi-topic analogues, have not been reported. $L_1^{2a}L_1^{2d}$ assemblies involve polymeric, not closed products.

3.2.2. A_2^{nA} and L_2^{nA} assemblies

Most assemblies containing two acceptor units generate 2-D polygons, although examples of 3-D polyhedra are also known. To the best of our knowledge, examples of only three polygon-generating descriptors are known: (i) $A_2^{2a}A_2^{2d}$, (ii) $L_2^{2a}A_2^{2d}$, and (iii) $A_2^{3a}A_2^{1d1d}L_2^{1d}$. $A_2^{2a}L_2^{2d}$ assemblies are unknown, while $L_2^{2a}L_2^{2d}$ assemblies cannot be closed. $A_2^{2a}A_2^{2d}$ and $A_2^{3a}A_3^{2d}$ assemblies which generate 3-D polyhedra also exist.

3.2.2.1. $A_2^{2a}A_2^{2d}$-based assemblies. Numerous $A_2^{2a}A_2^{2d}$ assemblies have been prepared. Most of these involve building blocks having 90° angles so that 2-D square structures are most prevalent. Other 2-D geometries are, however, also known, as are some 3-D structures.

A variety of hetero- and homotetrametallic $A_2^{2a}A_2^{2d}$ squares have been prepared by Stang and co-workers [17,18]. For example, the squares $[((dppp)M)_2(\mathbf{16})_2]^{4+}$ and $[((dppp)M)_2(\mathbf{17})_2]^{4+}$ (Scheme 11) (M = Pt, Pd; dppp = 1,3-bis(diphenylphosphino)propane) were obtained when the *cis*-triflated complexes **18a** and **18b** were treated with the kinetically stable donor units **16** and **17**, respectively. In these reactions the triflate coligands were coordinatively replaced by the cyano- or pyridyl- donors of **16** and **17**. The addition of silver triflate to the ethynylpyridine linked squares resulted in an unusual interaction; Ag^I ions became coordinated in a π-bonding mode to the two orthogonal acetylene groups at opposite corners of the square in a so-called "π-tweezer" effect. A square having four π-tweezers of similar structure is depicted in Scheme 32.

$A_2^{2a}A_2^{2d}$ squares containing T-shaped iodonium moieties at one set of opposite corners and di(phosphine)-

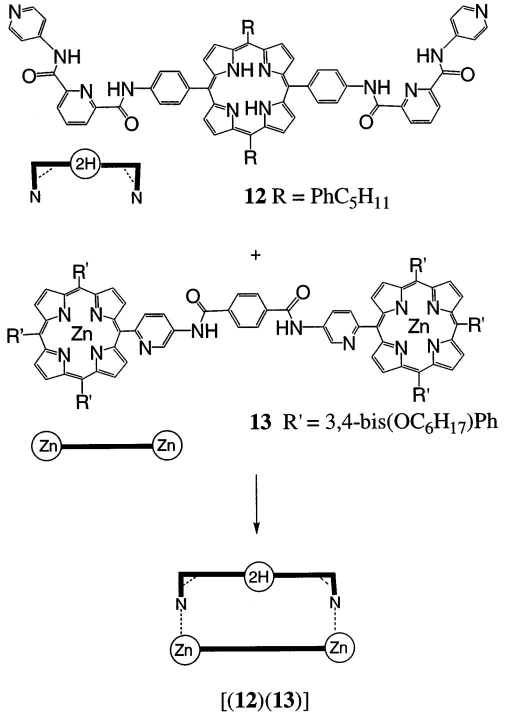

12 R = PhC$_5$H$_{11}$

13 R' = 3,4-bis(OC$_6$H$_{17}$)Ph

[(**12**)(**13**)]

Scheme 9.

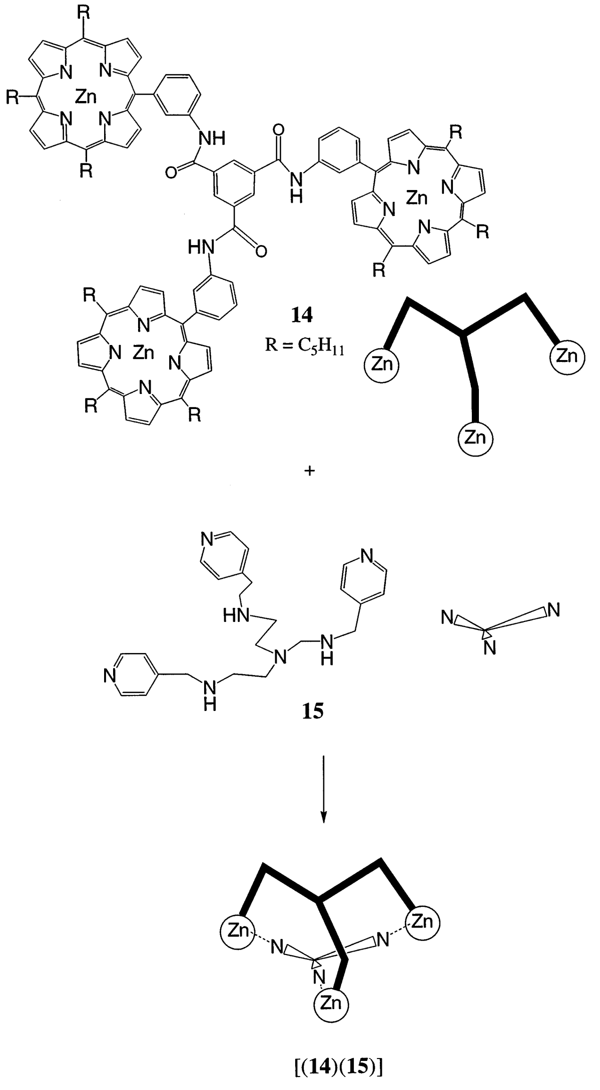

14
R = C$_5$H$_{11}$

15

[(**14**)(**15**)]

Scheme 10.

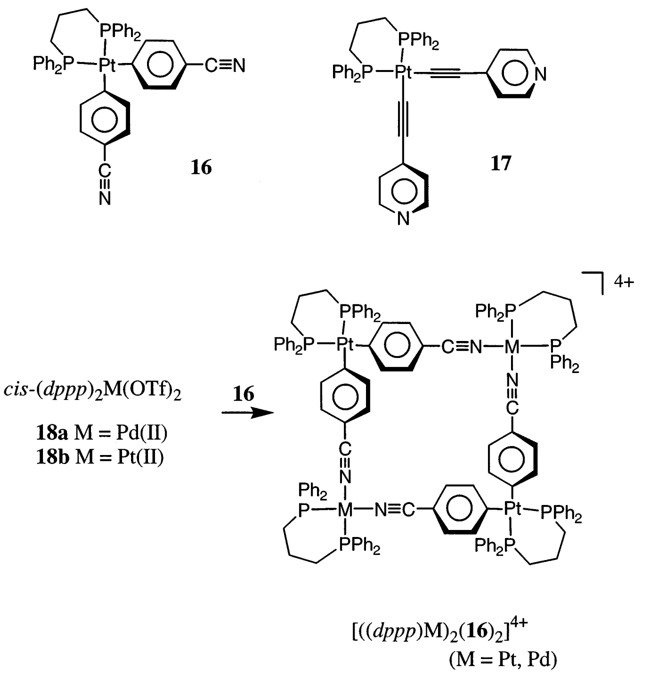

Scheme 11.

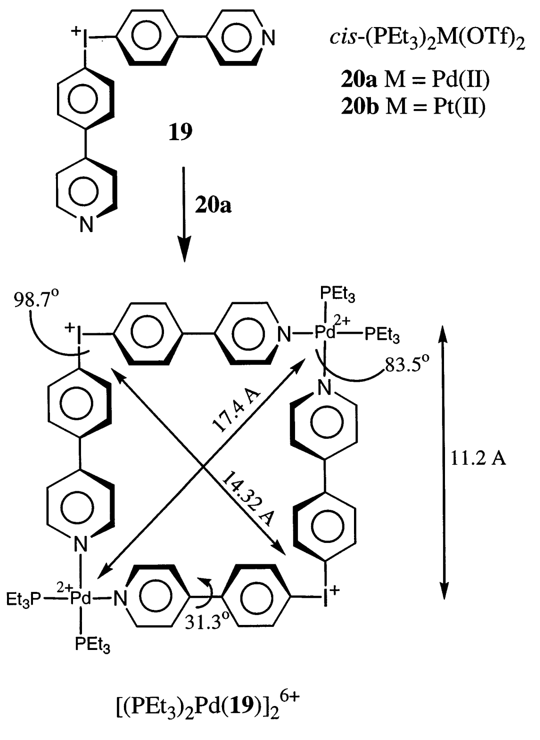

Scheme 12.

bound, square planar Pt^{II} or Pd^{II} metal ions at the other have also been prepared [19]. Scheme 12 illustrates one such assembly, $[(PEt_3)_2Pd(\mathbf{19})]_2^{6+}$. Similar compounds have been obtained using cyclic diamine co-ligands at opposite corners [20]. In the solid state these complexes typically have rhomboidal rather than square geometry owing to a distortion of the stereochemistry about the metal ions.

The use of an enantiomerically-pure chiral di(tertiary phosphine) (e.g. *R*- or *S*-binap; binap = 2,2′-bis(diphenylphosphino)-1,1′-binaphthyl) as the co-ligand on the corner metal sites of hybrid iodonium–Pt^{II} or Pd^{II} compounds resulted in the formation of optically active squares like $[((R\text{-binap})Pd)_2(\mathbf{21})_2]^{6+}$ depicted in Scheme 13 [21]. When the linker ligands are free to rotate (e.g. with 4-pyridyl binding sites on the iodonium moieties), the optical activity of such squares is due solely to the chirality of the metal–diphosphine auxiliaries. However, when linkers lacking rotational symmetry are used (e.g. iodonium moieties with 3-pyridyl binding sites), a mixture of helically-twisted diastereomers should theoretically be produced. In practice, asymmetric induction arising from the chirality of the auxiliaries resulted in the selective formation of only one of the six possible diastereomers [21].

Tetrametallic $A_2^{2a}A_2^{2d}$ squares $[((\text{binap})Pd)_2(R^*\text{-}\mathbf{23})_2]^{4+}$, which have different chiral di(tertiary phosphine) co-ligands on the metals at opposing sets of corners, were also prepared (Scheme 14) [22]. These compounds were generated by combining complex **23**, which contains *R*- or *S*-diop, with the bistriflate of (*R*- or *S*-binap)Pt^{II} or Pd^{II} **22a**/**b** (diop = 2,3-*o*-isopropylidene-2,3-dihydroxy-1,4-bis(diphenylphosphino)butane). Circular dichroism studies revealed that the chiroptical properties of the resulting squares were determined mainly by the binap rather than the diop moiety. This is in accord with the established chirality recognition

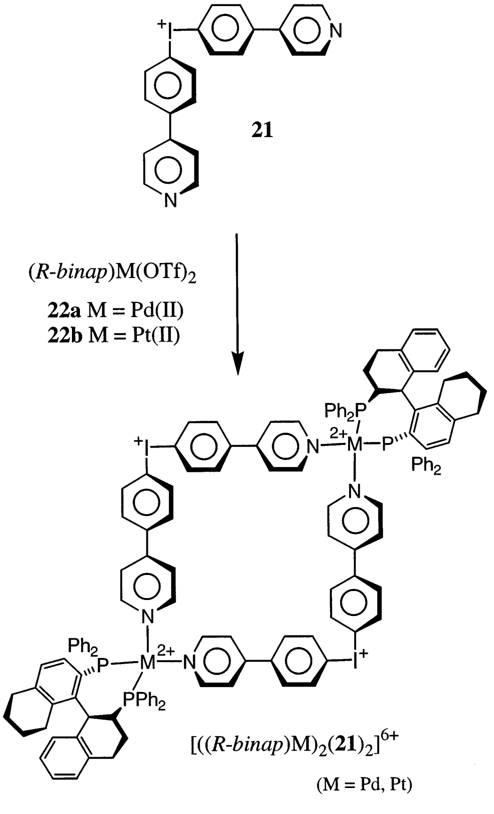

Scheme 13.

and induction abilities of these auxiliaries. The addition of two equiv. of Ag^I resulted in the formation of Ag–acetylene 'π-tweezer' complexes. A range of neutral mono- or bidentate guest, such as tetramethylpyrazine or phenazine, could be captured in the central cavity of the π-tweezer complex by simultaneous coordination of the two Ag^I ions [23].

A diastereomerically pure $A_2^{2a}A_2^{2d}$ square having *cis*-MoO_2^{2+} corners was generated by the self-assembly of a racemic mixture of the chiral spiro-linked di(catecholate) ligand **24** (Chart 1) with sodium molybdate [24]. The configuration of the octahedral metal centres in this molecule was controlled by the chirality of the rigid spiro-linker. In the solid state, the two enantiomers crystallised to form long microchannels down the axis perpendicular to the plane of the square. Other, conformationally more flexible $A_2^{2a}A_2^{2d}$ squares involving molybdenum–catecholate binding have also been reported [25].

A cationic $A_2^{2a}A_2^{2d}$ square assembly bearing tethered fullerenes has been prepared by the reaction of a bistriflated Pt^{II} complex with the dipyridylmethanofullerene ligand **25d** (Chart 1) [26]. In solution, a single structure of D_{2h} symmetry existed.

The reaction between *cis*-$Pt(PEt_3)_2(OTf)_2$ (**20b**) and a bis(4-pyridyl)carboxylate-substituted titanocene (**26**) (Scheme 15), resulted in the formation of the $A_2^{2a}A_2^{2d}$ square $[(PEt_3)_2Pt(\mathbf{26})]_2^{4+}$ having two titanocene and two Pt^{II} corners (OTf = triflate) [27].

When ligand **27** (Chart 1) was treated with Ru^{II}, it formed a kinetically stable Ru–P bound synthon having two unbound, pendant bipyridyl binding sites [28,29]. Treatment of this complex with Cu^I generated an $A_2^{2a}A_2^{2d}$ assembly.

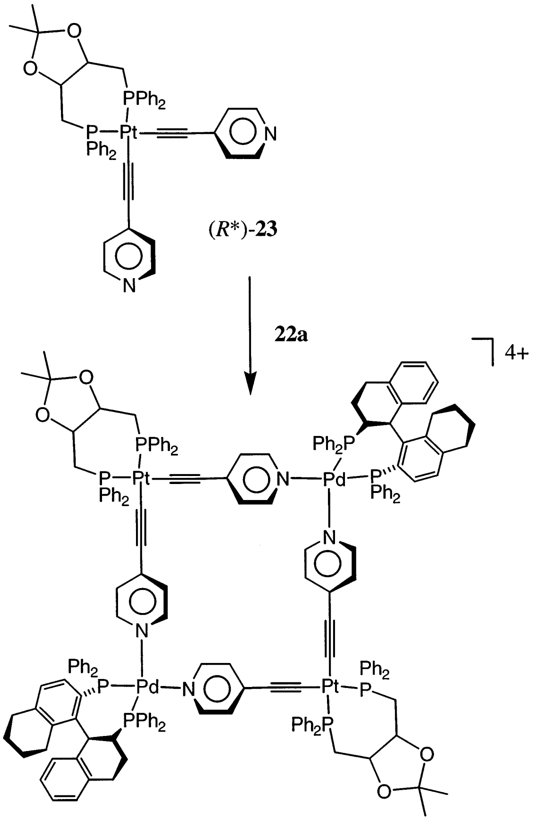

$[((R\text{-}binap)Pd)_2(R^*\text{-}\mathbf{23})_2]^{4+}$

Scheme 14.

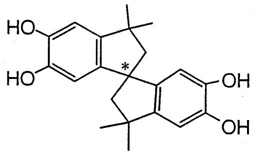

24 * chiral center

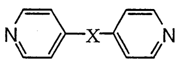

25a X = -C=C-
25b X = -C=C-C=C-
25c X = -p-C_6H_4-
25d X = C(fullerene)

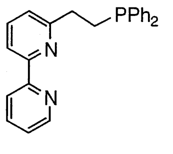

27

Chart 1.

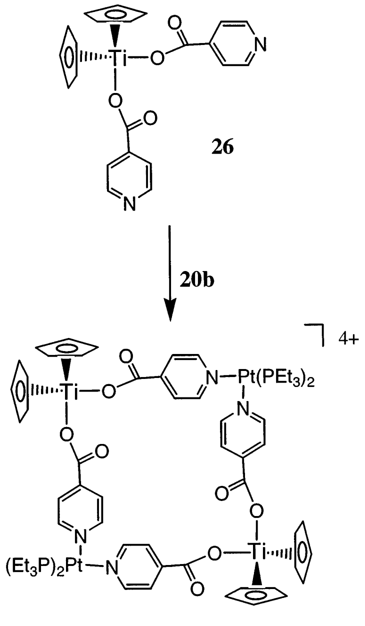

$[(PEt_3)_2Pt(\mathbf{26})]_2^{4+}$

Scheme 15.

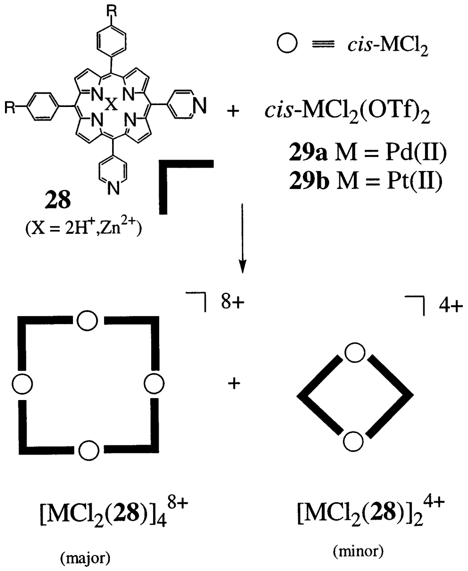

Scheme 16.

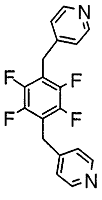

30

Chart 2.

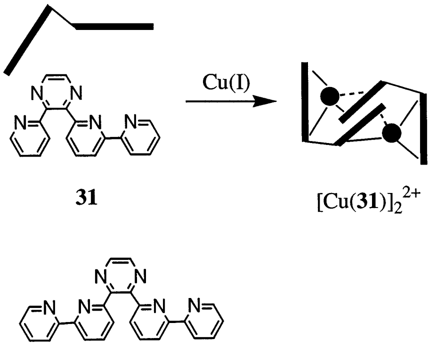

Scheme 17.

Spectroscopic evidence suggested the formation in low yield of the coordinatively unsaturated, porphyrin-bearing $A_2^{2a}A_2^{1a2d}$ square $[PdCl_2(\mathbf{28})]_2^{4+}$ (Scheme 16) when the L-shaped building block **28** (R = H) was titrated with *cis*-$[PdCl_2(OTf)_2]$ **29a** [30]. The $A_4^{2a}A_4^{1a2d}$ square $[PdCl_2(\mathbf{28})]_4^{8+}$ was the major product. Porphyrin-containing $A_2^{2a}A_2^{1a2d}$ squares have also been reported elsewhere [31]; it is possible that their corresponding $A_2^{2a}A_2^{2d}$ analogues were also formed in small quantities.

Other $A_2^{2a}A_2^{2d}$ assemblies include (i) a variety of silane-based rhomboids [32], (ii) squares having rhenium complexes as bridging units [33], and (iii) the water-soluble Pd^{II} complex of 1,4-bis(methyl(4-pyridine)-2,3,5,6-tetrafluorobenzene (**30**) (Chart 2) [34]. The latter cyclophane squares are electron-poor and therefore able to selectively host electron-rich compounds such as naphthalene. Rhenium-based squares typically display luminescence properties which are dependent on the guest present or which can be electrochemically manipulated [35a].

Several 3-D polyhedral $A_2^{2a}A_2^{2d}$ assemblies are known. When Cu^I is treated with 2-(2,2′-bipyridyl)-3-(2-pyridyl)pyrazine (**31**), the *racemic* $A_2^{2a}A_2^{2d}$ cyclophane box $[Cu(\mathbf{31})]_2^{2+}$ is formed (Scheme 17) [36]. The selective formation of the *racemic* diastereomer, rather than the *meso* compound obtained with **32** [37], may be due to favourable stacking interactions which exist both in the solid state or solution. The central cavity in $[Cu(\mathbf{31})]_2^{2+}$ had a height of 3.42–3.62 Å.

While not strictly a subject of this review, many double-stranded, bimetallic helicates can also be considered to be 3-D polyhedral $A_2^{2a}A_2^{2d}$ assemblies.

3.2.2.2. $L_2^{2a}A_2^{2d}$ *assemblies*.

$L_2^{2a}A_2^{2d}$ assemblies are somewhat unusual since they necessarily involve ligands which cumulatively subtend a 360° angle between their binding sites; $A_1^{2a}A_1^{2d}$ assemblies have a similar requirement (Section 3.2.1). Examples of $L_2^{2a}A_2^{2d}$ ensembles include (i) the molecular square $[Fe_2(\mathbf{33})_2]^{8+}$ (Scheme

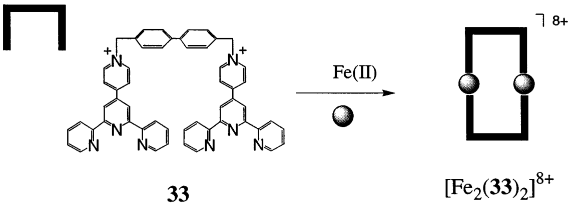

Scheme 18.

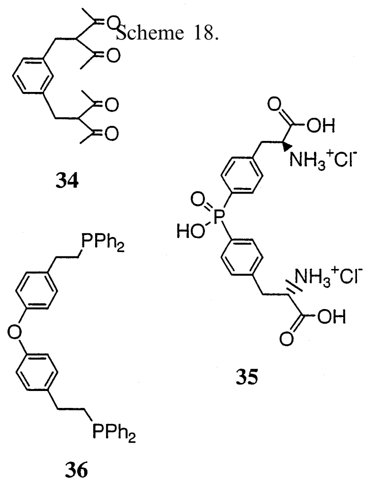

Chart 3.

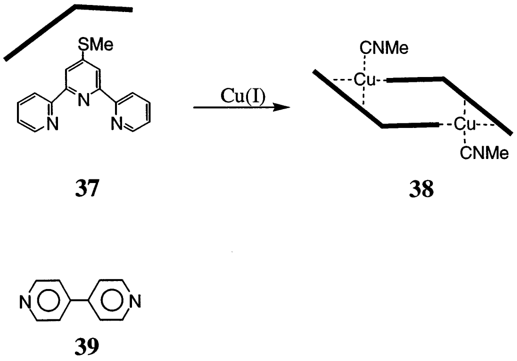

Scheme 19.

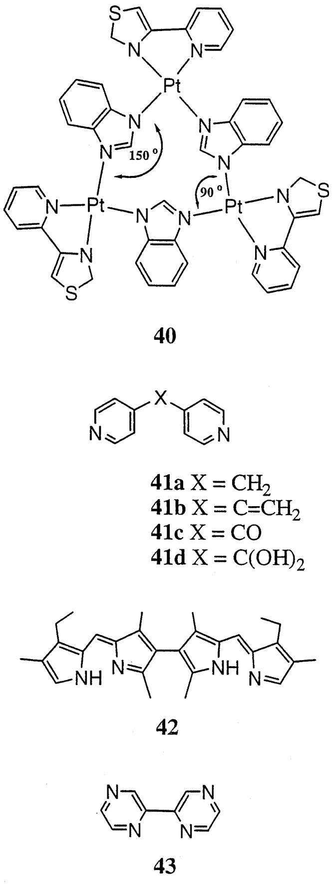

41a X = CH_2
41b X = $C{=}CH_2$
41c X = CO
41d X = $C(OH)_2$

Chart 4.

18) [38], (ii) squares comprising Cu^{II} and the ligand **34** (Chart 3) (and its naphthalene linked analogue) [39], (iii) various transition metal metallocycles of ligand **35** (Chart 3) [40], (iv) certain Ag^{I}-diazacycles [20], (v) the Ag^{I} complex of 1,4-bis(2-pyridoxy)benzene [41], and (vi) dimeric Pd^{II}-**36** metallocycles [42]. In the molecular squares described above, the metal ions are the linear components and the ligands the angled components. Ligands **33** and **34** along with **12**, are rare examples of angular building blocks which can rigidly and squarely subtend an angle of 360°.

3.2.2.3. $A_2^{3a}A_3^{2d}$ assemblies. A series of novel and rather stable 3-D $A_2^{3a}A_3^{2d}$ cyclophane boxes have been self-assembled by the reaction of a tris(Zn^{2+}–cyclen)(Zn_3L^1) complex (L^1 = 1,3,5-tris(1,4,7,10-tetraazacyclododecan-1-ylmethyl)benzene) with di- or tri-deprotonated cyanuric acid (cyclen = 1,4,7,10-tetraazacyclododecane) [43].

3.2.2.4. $A_2^{3a}A_2^{1d1d}L_2^{1d}$ assemblies. An unusual $A_2^{3a}A_2^{1d1d}L_2^{1d}$ molecular square(**38**) (Scheme 19) containing a central cyclophane cavity was obtained by the reaction of terpyridine ligand **37** with $[Cu(MeCN)_4]^+$ in acetonitrile [44]. Cadmium(II) and silver(I) have been successfully employed in similar processes [45]. The above reaction contrasts with that of 4,4′-bipyridine, **39**, and $[Cu(MeCN)_4]^+$ in which the absence of an ethylene diamine or another blocking ligand on the metal resulted in the formation of polymeric arrays. The structure of **38** in solution was confirmed by mass spectrometry, cyclic voltammetry and ^1H-NMR. Polymers containing cyclophane cavities of this type within their backbone were also obtained when **37** was combined with Ag^{I} in the absence of acetonitrile.

3.2.3. A_3^{na} and L_3^{na} assemblies

2-D Polygons involving tritopic acceptor units have been generated in the following types of self-assembly: (i) $A_3^{2a}A_3^{2d}$, (ii) $A_3^{2a}L_3^{2d}$, and (iii) $L_3^{2a}A_3^{2d}$. Tritopic metals have also been employed in the formation of 3-D polyhedra having the descriptor $A_3^{2a}A_2^{3d}$. Examples of $L_3^{2a}A_2^{3d}$ and $A_3^{2a}L_2^{3d}$ assemblies are unknown.

3.2.3.1. $A_3^{2a}A_3^{2d}$ assemblies. Self-assembled $A_3^{2a}A_3^{2d}$ compounds typically adopt a 2-D triangular or hexagonal shape; a variety of such assemblies are known. For example, the self-assembly of three right-angled angular units with three other angular units each subtending an angle of 150° may give a complex closely resembling a molecular triangle. Thus, the bowl-shaped, luminescent, $A_3^{2a}A_3^{2d}$ complex **40** (Chart 4) was obtained as an approximate molecular triangle in high yield from the corresponding *N*-deprotonated anion of benzimidazole [46]. Similar triangles have been formed using various nucleobases [47].

An $A_3^{2a}A_3^{2d}$ hexagon $[(en)Pd(\mathbf{41b})]_3^{6+}$ has also been formed in the reaction of **41b** with *cis*-(en)Pd^{II} **44** (en = 1,2-ethylenediamine) in aqueous medium at room temperature (Scheme 20) [48]. The product mixture included the $A_3^{2a}A_3^{2d}$ hexagon (27%), the $A_2^{2a}A_2^{2d}$ square $[(en)Pd(\mathbf{41b})]_2^{4+}$ (53%), and coordination oligomers (20%). The formation of this molecule is an interesting example of competing effects in the self-assembly of metallocycles. Hexagon formation is promoted by **41b** which binds at a 120° angle. However, the directing angle of square planar Pd^{II} is 90°, which is better suited to square formation. Since the square existed in greater

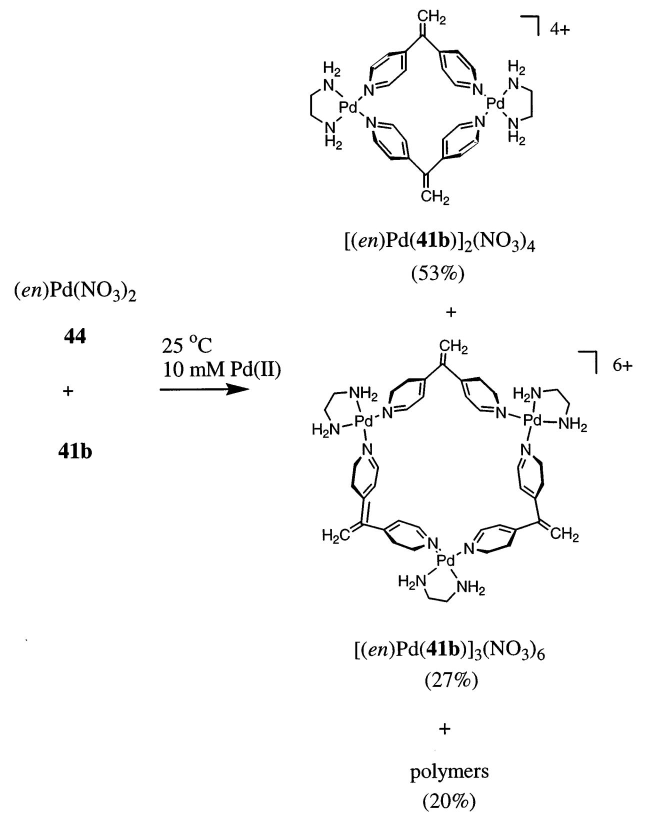

Scheme 20.

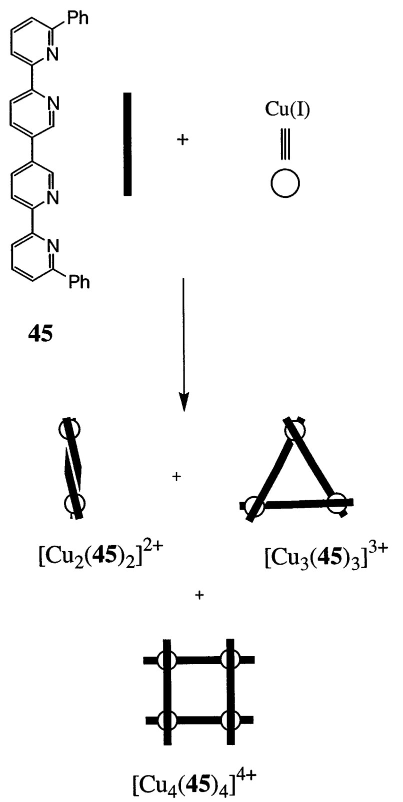

Scheme 21.

proportions than the hexagon under the conditions of the above experiment, the stereochemical preferences of the metal complex appear to dominate those of the ligand. Interestingly, the relative proportion of the hexagon increased as the mixture was concentrated, suggesting that the difference in the thermodynamic stabilities of the square and hexagon was of the same order as the entropic effect favouring the hexagon over the square. The angles subtended by the methyl-bridged bis(4-pyridyl) ligands **41** can be conveniently adjusted by alterations to the substituents on the bridging methylene carbon. Thus, **41a** exhibits a directing angle of 109° when binding, while **41b**–**c** bind at 120° [48].

A range of other $A_3^{2a}A_3^{2d}$ hexagons have been prepared [49], as have organometallic hexagons incorporating Hg^{II} with nucleobases [50,51] and Fe^{III} with triethanolamine (giving [12]metallocrown-6 structures with occupied or unoccupied cavities) [52].

3.2.3.2. $A_3^{2a}L_3^{2d}$ assemblies. Because of the presence of the three linear components, $A_3^{2a}L_3^{2d}$ assemblies are generally triangular in shape, although examples of $A_3^{2a}L_3^{2d}$ hexagons are known.

$A_3^{2a}L_3^{2d}$ assemblies have been reported when: (i) (1,4,7-triazacyclononane)Cu^{II} is treated with deprotonated imidazole [53], (ii) Zn^{II} or Co^{II} reacts with ligand **42** (Chart 4) [54], (iii) Pt^{II} or Pd^{II} binds 2,2′-bipyrazine **43** (Chart 4) [55], and in low yield when (iv) (ethylenediamine)Pd^{II} is treated with **25a**–**c** (Chart 1) [48,56a]. While molecular triangles are obtained for (i)–(iii) above, certain of the complexes in (iv) have an overall hexagonal structure. Luminescent triangular $A_3^{2a}L_3^{2d}$ complexes having Re^{I} corner units have also been reported [57].

Many $A_3^{2a}L_3^{2d}$ assemblies exist in a thermodynamic equilibrium with other, competing self-assembled products. For example, the $A_3^{2a}L_3^{2d}$ triangle $[Cu_3(\mathbf{45})_3]^{3+}$ was formed from Cu^{I} and **45** as 30% of an equilibrium mixture, which included the helicate $[Cu_2(\mathbf{45})_2]^{2+}$ and the grid $[Cu_4(\mathbf{45})_4]^{4+}$ (Scheme 21) [58]. Other $A_3^{2a}L_3^{2d}$ triangles exist in an equilibrium with their competing $A_2^{2a}L_2^{2d}$ squares [56a]. In these cases the triangles have been favoured over their squares by the presence of: (a) flexible linkers between the ligand binding sites, (b) sterically demanding co-ligands, (c) certain guest molecules which bring about induced-fit molecular recognition, or (d) increased solution concentrations [56a,59]. As the triangles contain six component building blocks (compared to the four in squares), an increase in the solution concentration entropically supplements their overall thermodynamic stability.

3.2.3.3. $L_3^{2a}A_3^{2d}$ assemblies. Treatment of octahedral Fe^{II} with the alkyne segmented octapyridino ligand **46** (Scheme 22), which has a 60° bite angle, led to the formation in 74% yield of the $L_3^{2a}A_3^{2d}$ assembly

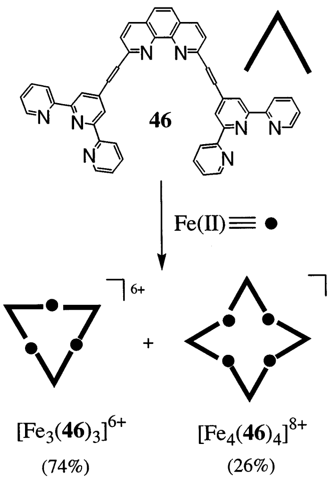

Scheme 22.

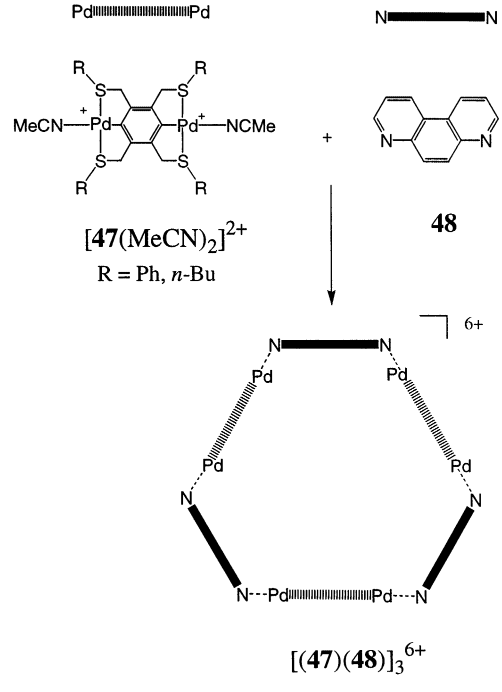

Scheme 23.

$[Fe_3(\mathbf{46})_3]^{6+}$ [60]. The composition of this triangular complex was determined using electrospray mass spectrometry, which also revealed the presence of the corresponding $A_4^{2a}A_4^{2d}$ polygon in 26% yield (Section 3.2.4.1).

The $L_3^{2a}A_3^{2d}$ hexagon $[(\mathbf{47})(\mathbf{48})]_3^{6+}$ was obtained by the reaction of 4,7-phenanthroline **48** (directing angle: 60°) with the linear dipalladium complex $[\mathbf{47}(MeCN)_2]^{2+}$ (Scheme 23) [61]. The phenanthroline N–N distance (7.80 Å) is comparable to the Pd···Pd distance within the organopalladium unit (6.83 Å), thereby generating the overall hexagonal shape.

3.2.3.4. $A_3^{2a}A_2^{3d}$ assemblies. Because of the mismatch between the topicity of the acceptor-based units and that of the donor-based units, $A_3^{2a}A_2^{3d}$ assemblies are necessarily 3-D. Several $A_3^{2a}A_2^{3d}$ cyclophane boxes have been prepared. These include $[(Pd(en))_3((\mathbf{49})_2]^{6+}$ (Scheme 24) which was obtained by the reaction of the tridentate ligand 1,3,5-tris(4-pyridylmethyl)benzene (**49**) with $(en)Pd(NO_3)_2$ (**44**) in the presence of an aromatic guest, such as (4-methoxyphenyl)acetic acid [62]. This reaction involved an induced-fit molecular recognition process since $[(Pd(en))_3((\mathbf{49})_2]^{6+}$ was obtained only in the presence of the guest. Without the guest, poorly defined oligomeric complexes were obtained instead. These spontaneously converted to the cyclophane box upon addition of the guest.

$A_3^{2a}A_2^{3d}$ cyclophane boxes were also obtained when square planar Pt^{II} or tetrahedral Cu^{I} metal ions were treated with ligands containing a central benzene ring substituted with diphenylphosphine- (**50**; Scheme 25) [63] or bis(isoquinoline)- (**51**; Fig. 4) [64] groups, respectively.

3.2.4. A_4^{na} and L_4^{na} assemblies

Numerous A_4^{na} and L_4^{na} assemblies are known. In cases where these involve only ditopic ligands, 2-D polygonal structures—primarily squares—are formed. Descriptors for such procedures include $L_4^{2a}A_4^{2d}$ and $A_4^{2a}L_4^{2d}$. An $A_4^{2a}A_4^{2d}$ star-type assembly has also been reported. The use of tri- or multi-topic building blocks induces the formation of 3-D polyhedra. Known compounds of this type involve a tetrahedron of metal ions about a central cavity and exhibit the descriptors: (i) $A_4^{3a}A_6^{2d}$, (ii) $A_4^{3a}L_6^{2d}$, (iii) $A_4^{3a}A_4^{3d}$, (iv) $A_4^{2a}A_2^{4a}A_8^{1d1d}$, or (v) $A_4^{2a}A_1^{8d}$.

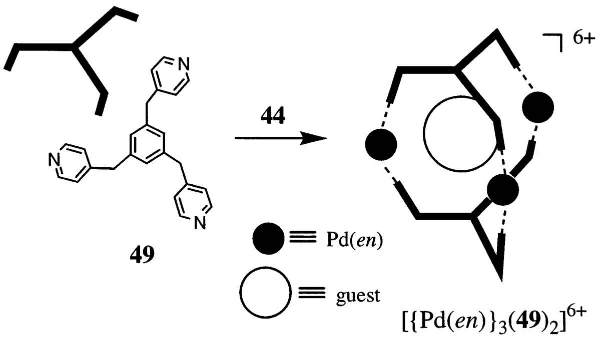

Scheme 24.

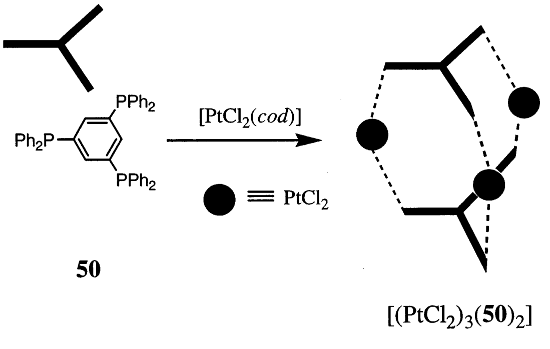

Scheme 25.

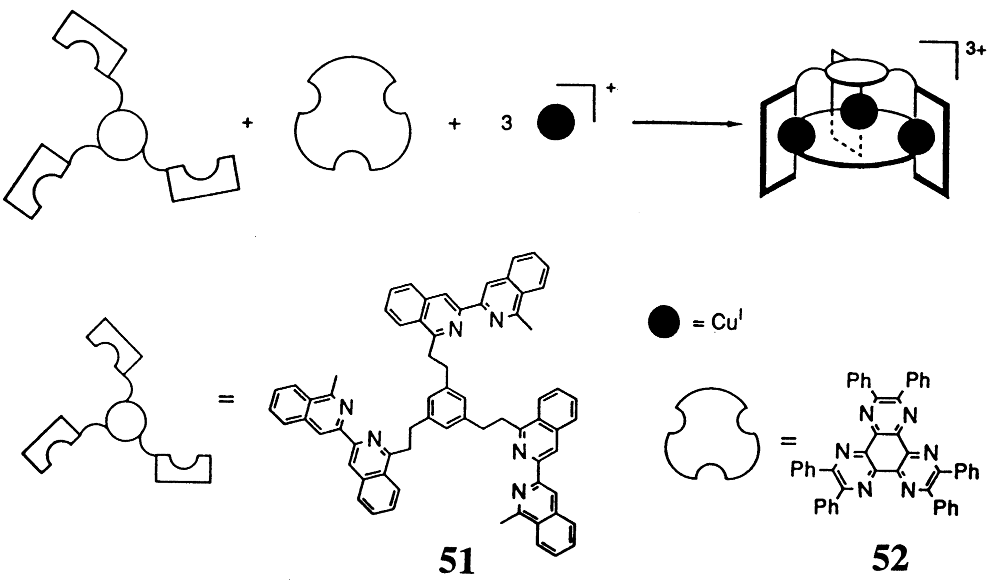

Fig. 4. Self-assembly of a cyclophane box. (Reproduced with permission; Ref. [64]. Copyright 1993 the Royal Society of Chemistry.)

3.2.4.1. $A_4^{2a}A_4^{2d}$ and $A_4^{2a}L_4^{2d}$-based assemblies

$A_4^{2a}A_4^{2d}$ assemblies. From electrospray mass spectrometric evidence, the $A_2^{2a}A_2^{2d}$ star assembly $[Fe_2(\mathbf{46})_2]^{4+}$ has been proposed to form in low yield in the reaction of **46** with Fe^{II} depicted in Scheme 22 (see Section 3.2.2.1) [60]. To the best of our knowledge no other $A_4^{2a}A_4^{2d}$ assemblies are known.

$A_4^{2a}L_4^{2d}$-based assemblies. $A_4^{2a}L_4^{2d}$ molecular squares are possibly the most well-known of the coordination polygons. Numerous such assemblies have been prepared by the combination of square planar metals with linear bidentate ligands having donor sites at each end.

Two $A_4^{2a}L_4^{2d}$ square assemblies are illustrated in $[Pd(en)(\mathbf{39})]_4^{8+}$ and $[Pd(dppp)(\mathbf{39})]_4^{8+}$, respectively (Scheme 26) [56,65]. In these cases, the rigid ditopic ligand 4,4′-bipyridine, **39**, (illustrated in Scheme 19) was self-assembled with biphosphine- or diamine-bound square planar Pd^{II} or Pt^{II}. NMR studies confirmed the presence of the square architectures in solution. The biphosphine-containing square was soluble in organic solvents, while its diamine analogue was water soluble.

As in the formation of some of the $A_2^{2a}L_2^{2d}$ squares described above, the chelating co-ligands on the metal ions are required to occupy two *cis*-coordination sites on the metal ions in order to ensure that a 90° angle is formed by the metal. Monodentate co-ligands, such as the PEt$_3$ ligands in **20**, can also perform this function as long as they remain *cis*-coordinated during the reaction.

In the reaction of 1,4-dicyanobenzene **54a** or 4,4′-dicyanobiphenyl **54b** with metal ions, cationic $A_4^{2a}L_4^{2d}$ squares were self-assembled with Pd^{II} but not with Pt^{II} which instead formed oligomeric products (Scheme 27) [65]. This may have been due to the kinetic inertness of Pt–NC bonds. However the authors suggested that the absence of stabilising π-stacking interactions may also have played a role. While the analogous bipyridyl squares were kinetically inert, the cyano-squares were labile in solution. Treatment of the cyano-squares with **39** therefore resulted in conversion to their bipyridyl analogues. The squares formed host–guest interactions with electron-rich molecules, such as 1,5-dihydroxynaphthalene, in solution.

Diastereomerically pure tetranuclear $A_4^{2a}L_4^{2d}$ molecular squares were obtained in the reaction of the bis(triflates) of (*R*)-(+)-binap Pd^{II} (**22a**) or Pt^{II} (**22b**) with 2,6-diazaanthracene **55** in acetone at room temperature (Scheme 28) [66]. $^{31}P\{^1H\}$-NMR spectroscopy indicated that all of the diaza ligands, which do not possess rotational symmetry, were restricted in their rotation within the product. Six diastereomers, involving differently twisted arrangements of **55** in the complex, were therefore possible. However the helically-twisted *anti*-diastereomer was selectively formed. When 2,6-diazaanthracene-9,10-dione **56** was used as the linker, small but detectable amounts of the other diastereomers were also obtained. The use of (*S*)-(−)-*binap* co-ligands resulted in the formation of the mirror image products, while achiral phosphine co-ligands produced mixtures of the possible diastereomers [66]. In comparison to the optically active, hybrid iodonium-transition metal $A_2^{2a}A_2^{2d}$ square assemblies described earlier (Section 3.2.2.1), the tetrametallic $A_4^{2a}L_4^{2d}$ squares were formed in greater diastereomeric excess and were conformationally more rigid [66]. This was thought to be due to increased rotational inhibition, arising from the coordination of each linker ligand to two metal ions in the tetrametallic squares, rather than just one in the hybrid squares.

$A_4^{2a}L_4^{2d}$ molecular squares which contain crown ethers or calixarenes, such as **57**, have been self-assembled by incorporation of these moieties within the biphosphine co-ligands attached to the corner metal ions (Fig. 5) [67]. Since crown ethers are excellent hosts for hard metals and calixarenes have an affinity for neutral guests, the presence of these moieties extends the possible function of molecular squares. Studies indicated that the calixarene squares were, for example, able to transport organic sulfonate ions from one aqueous layer through a chloroform phase to another aqueous layer in a U-tube apparatus [67]. The use of bis(diphenylphosphino)ferrocene as a co-ligand has similarly permitted the inclusion of redox active components in molecular squares of this type (e.g. **58** in Scheme 29) [68].

$A_4^{2a}L_4^{2d}$-based molecular squares incorporating porphyrins have also been prepared. Porphyrins may act as linear [30,31,69] building blocks when 4-pyridines, which have been substituted onto the porphyrin scaffold, orthogonally coordinate separate metal ions in the manner depicted in **60** (Scheme 30) [69]. When X = 2H$^+$, **60** has the descriptor $A_4^{2a}L_4^{2d}$. However when X = Zn^{2+}, **60** is a coordinatively unsaturated $A_4^{2a}L_4^{1a2d}$ assembly. Porphyrin-containing molecular squares of this type which incorporate between four and eight metal ions have been reported [31]. Several of these were made chiral by the use of enantiomerically-pure, chiral di(phosphine) co-ligands on the corner metal ions.

cis-[M(*en*)(OTf)$_2$]

53a M = Pd(II)
53b M = Pt(II)

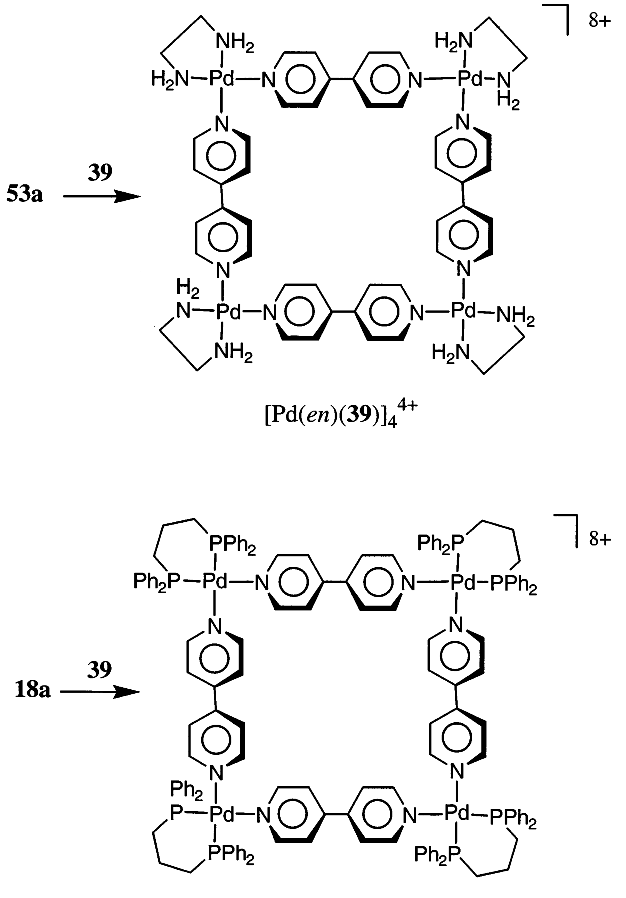

[Pd(*en*)(**39**)]$_4^{4+}$

[Pd(*dppp*)(**39**)]$_4^{8+}$

Scheme 26.

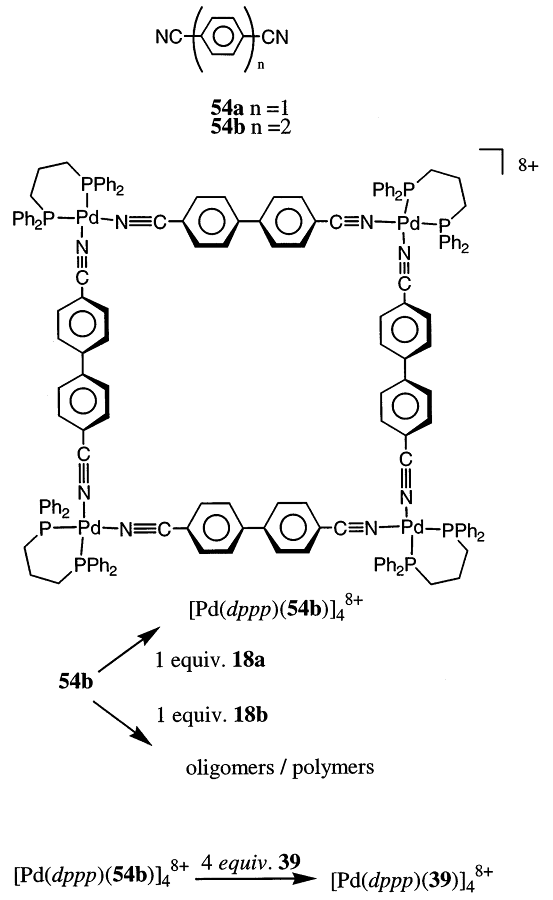

54a n = 1
54b n = 2

[Pd(*dppp*)(**54b**)]$_4^{8+}$

54b
1 equiv. **18a**
1 equiv. **18b**
oligomers / polymers

[Pd(*dppp*)(**54b**)]$_4^{8+}$ $\xrightarrow{4\ equiv.\ \mathbf{39}}$ [Pd(*dppp*)(**39**)]$_4^{8+}$

Scheme 27.

$A_4^{2a}L_4^{2d}$ square and rectangular assemblies involving rhenium ions as the corner components [35,57,70,71] have also been prepared, as have grid-like squares involving Co$^{II/III}$ with tetra(2-pyridyl)thiocarbazide **(61)** or 1-(2-thiouracil-4-methylene)-3,6-diazahexane **(62)** (Chart 5) [72,73]. As noted earlier, rhenium-based squares may display luminescence properties which vary depending on the guest present; their overall luminescence properties may also be electrochemically altered in a stepwise manner [35a].

3.2.4.2. $L_4^{2a}A_4^{2d}$ assemblies. If the ligands and metals in $A_4^{2a}L_4^{2d}$ assemblies (Section 3.2.4.1) could be interchanged, an $L_4^{2a}A_4^{2d}$ assembly would be generated. $L_4^{2a}A_4^{2d}$-type molecular squares have been prepared us-

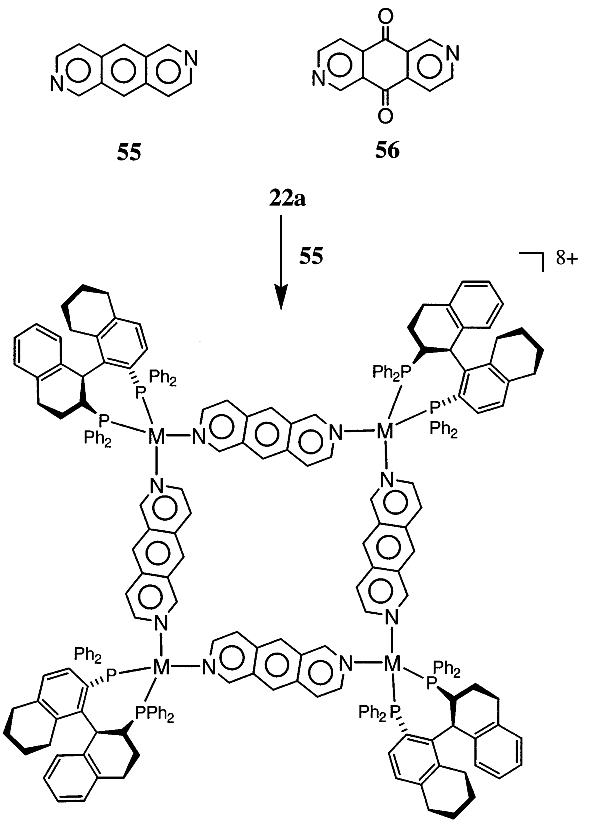

$[(R\text{-}binap)M(\mathbf{55})]_4^{8+}$ M = Pd, Pt

Scheme 28.

ing porphyrins orthogonally substituted with 4-pyridines [30,31] as in the formation of **64** (Scheme 31) [30]. Molecular squares of this type can incorporate four or eight metal ions, depending on whether the porphyrins are metallated or not [31]. When $X = 2H^+$, **64** has the descriptor $L_4^{2a}A_4^{2d}$. However, when $X = Zn^{2+}$, **64** is coordinatively unsaturated and has the descriptor $L_4^{2a}A_4^{1a2d}$.

$L_4^{2a}A_4^{2d}$ squares of nanometer dimensions—termed nanosquares—have been prepared in the reaction of the *cis*-substituted bis(ethynylpyridine) Pt^{II} diphophosphine complex **17** with the triflated linear di(platinum) complex **65** (Scheme 32) [74]. T-shaped bis(4-pyridyl) iodonium species have also been used as corner units, as have substituted porphyrins [31]. The sides of these squares ranged from 2.6 to 3.4 nm in length. Treatment with Ag^I resulted in the π-tweezer host–guest interactions shown at the corners of **66** [74]. While formally classified as $L_4^{2a}A_4^{2d}$, these squares contain eight or twelve metal ions.

The $A_4^{2a}L_4^{2d}$ [4]metallacalixarene **68** (Scheme 33) is formed as a kinetically stable entity by the interaction of four uracil moieties with chelated Pt^{II} at elevated pH. It can be considered a molecular square, although when treated with labile transition metal ions a 3-D rectangular box is formed (see Section 3.2.4.7) [75].

3.2.4.3. $A_4^{3a}A_6^{2d}$ assemblies. The combination of four tritopic A^{3a} metal ions with six ditopic A^{2a} ligands can only lead to coordinative saturation when a 3-D adamantanoid-like structure is formed. Such structures involve a tetrahedra of metal ions with the ligands occupying the connecting edges (Fig. 6(a)). In the closely related $A_4^{3a}L_6^{2d}$ assemblies (Section 3.2.4.4), the ligands cannot be angled, so that only a true tetrahedron of the type illustrated in Fig. 6(b) can be generated. $A_4^{3a}A_6^{2d}$ assemblies are also related to $A_6^{2a}A_4^{3d}$ assemblies (Section 3.2.5.2) by an interconversion of the metals and ligands present; they consequently share many symmetry properties.

Raymond and co-workers have prepared a series of tetranuclear adamantanoids and tetrahedra using their symmetry-interaction approach [76], which rationalises the formation of such polyhedra by the combination of a ligand having two-fold symmetry (such as a suitable hydroxamate) with an octahedral metal centre having three-fold symmetry (such as trivalent gallium or iron) [77]. The reaction of Ga^{III} with the pre-designed bis(hydroxamate) ligand $\mathbf{70}^{2-}\cdot 2H^+$ produced the tetrahedral adamantanoid $[Ga_4(\mathbf{70})_6]$ for example (Scheme 34) [77]. In the solid state this complex displayed S_4 symmetry, however ^{1}H-NMR spectroscopy established that all the ligands in the cluster were equivalent in solution, indicating T-symmetry. No exchange occurred on the NMR time-scale between cluster ligands and free, unbound ligands in solution. This suggests exceedingly slow, or possibly even non-existent kinetics. It is possible that these boxes may have been formed in an irreversible kinetically-guided process. Other boxes of this type have been prepared by the same researchers; these involved ligand **71** with Ga^{III} and Fe^{III} [78,79]. Polyhedra of this type are able to selectively encapsulate small cationic guests within the central cavity in an entropy-driven process.

A variety of tetranuclear $A_4^{3a}A_6^{2d}$ tetrahedra have also been prepared by Saalfrank and co-workers; these include the neutral compound $[Fe_4(\mathbf{72b})_6]$ depicted in Fig. 7 which was formed in the self-assembly of the deprotonated bis(methyl acetoacetate) derivative **72b** with Fe^{III} [80]. Two enantiomeric pairs, Δ-/Λ-*fac* and Δ-/Λ-*mer*, are theoretically possible in this complex. In this case an exact S_4 symmetry was obtained in the solid state, meaning that the achiral *meso*-diastereomer was selectively formed (i.e. one pair of metal centres had a Λ-configuration, while the others were Δ). This result contrasts with most of the other tetrahedra and tetranuclear adamantanoids prepared by these authors which were obtained as anionic chiral T-symmetric products using Mg^{II}, Mn^{II}, Co^{II}, Ni^{II}, and Fe^{III}/Fe^{II} [81–83]. The latter, mixed-valence tetrahedra, $(NH_4)[Fe_4(\mathbf{73})_6]$ (Scheme 35), were particularly interesting; in the solid state their central cavities contained an endohedrally complexed ammonium cation for charge compensation. The other complexes studied had exchangeable exohedral cations

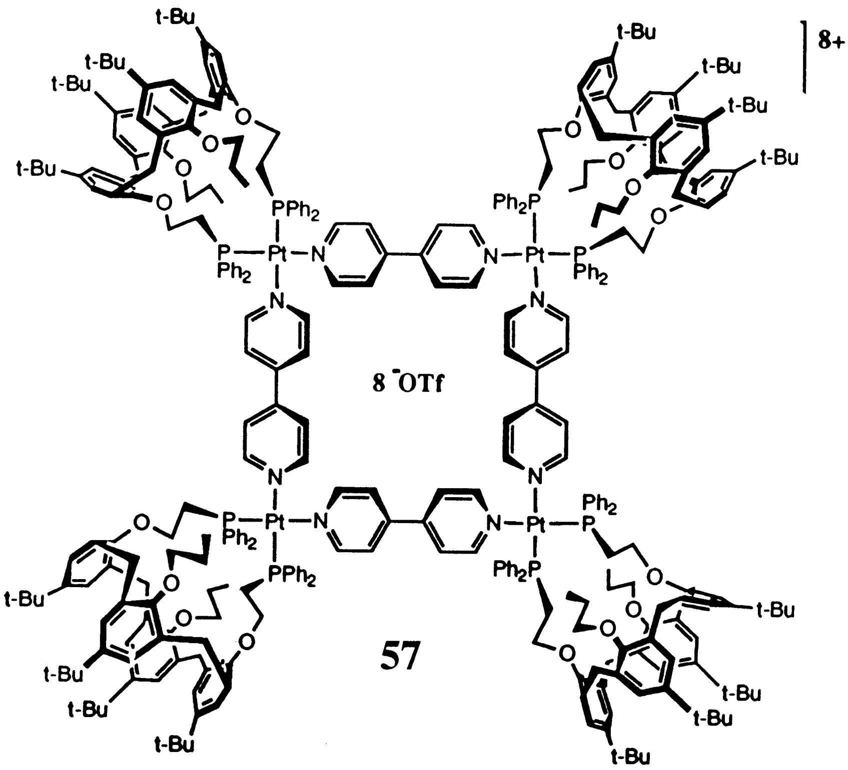

57

Fig. 5. A molecular square containing calixarene functionalities. (Reproduced with permission from Ref. [67]. Copyright 1997, American Chemical Society.)

[84]. Their high symmetry and preparative yields suggests that these molecules were formed via a thermodynamic equilibrium, although their kinetic lability has not been determined.

The reaction of the (*S*,*S*)-bis(catecholamide) ligand **74c** with Ga^{III} also produces a *T*-symmetric $A_4^{3a}A_6^{2d}$ adamantanoid (Scheme 36) [85]. The specificity of this reaction is remarkable: the observed isomer, in which each metal displays a Λ-configuration, would comprise only 1/16th of a statistical mixture. The formation of a pair of mirror-image tetrahedral adamantanoids from the *racemic* form of **74c**, therefore occurred selectively from 112 theoretically possible variants. The same reaction with the derivative ligands **74a**–**b** and **74d** produced helicates.

Other tetranuclear boxes of these types have also been reported [86].

3.2.4.4. $A_4^{3a}L_6^{2d}$ *assemblies.*

$A_4^{3a}L_6^{2d}$ assemblies are closely related to $A_4^{3a}A_6^{2d}$ assemblies (Section 3.2.4.3) in that they have the same combination of building blocks. In this case however, the donor ligands are not angled, but rigidly linear. This means they must lie on the connecting edges of the tetrahedron of metal ions as depicted in Fig. 6(b). In so doing, they preserve the overall tetrahedral shape of the cluster rather than generating the adamantanoid shape of many $A_4^{3a}A_6^{2d}$ assemblies (Fig. 6(a)).

The $A_4^{3a}L_6^{2d}$ tetrahedron, $[((\text{triphos})\text{Fe})_4(\mathbf{75})_6]^{8+}$ (Scheme 37), has been prepared using triphos, $Fe(BF_4)_2$, and the dicyanoethane, **75** (triphos = 1,1,1-tris(diphenylphosphinomethane)ethane) [87]. While **75** is not strictly linear, the rigidity of the central ethene linkage ensures a near-linear bonding arrangement between the ligand and the two metal ions it connects. In the solid state this box encapsulates a BF_4^- anion in its central cavity.

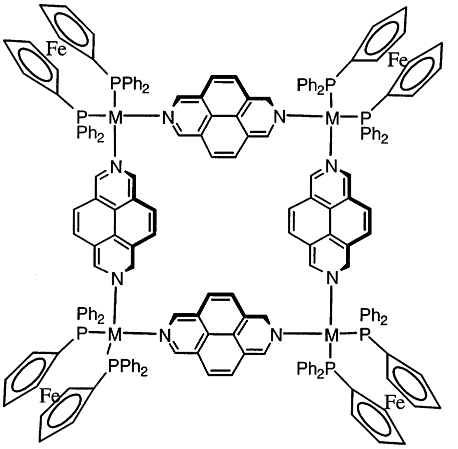

58a M = Pd
58b M = Pt

Scheme 29.

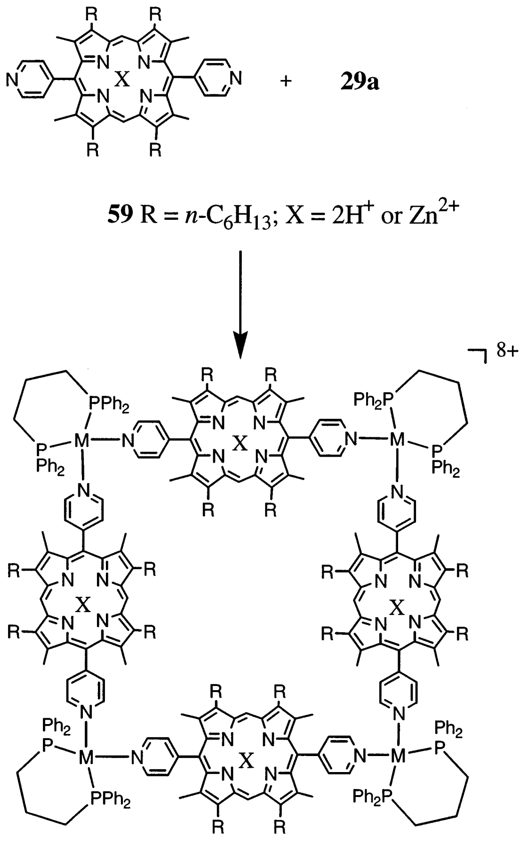

59 R = *n*-C_6H_{13}; X = $2H^+$ or Zn^{2+}

60

Scheme 30.

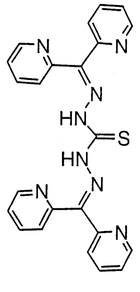

61

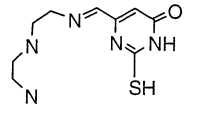

62

Chart 5.

3.2.4.5. *$A_4^{3a}A_4^{3d}$ assemblies*. The highly symmetrical compound $[Ti_4(\mathbf{76})_4]^{8-}$ (Scheme 38) which was recently prepared by Raymond and co-workers, is a face-occupied $A_4^{3a}A_4^{3d}$ tetrahedron of the type illustrated in Fig. 6(c) [88a]. Electrospray mass spectrometry indicated that $[Ti_4(\mathbf{76})_4]^{8-}$ also existed in solution and rapidly exchanged NH_4^+ counter-ions [88a,88b]. The lack of fragmentation suggested the anion to be highly stable; this was likely due to the inert nature of the Ti^{IV}–catecholate interactions and the fact that this structure was the only arrangement able to satisfy simultaneously the

trans-$[MCl_2(NCPh)_2]$

63a M = Pd(II)
63b M = Pt(II)

28 + **63a**
(R=H)

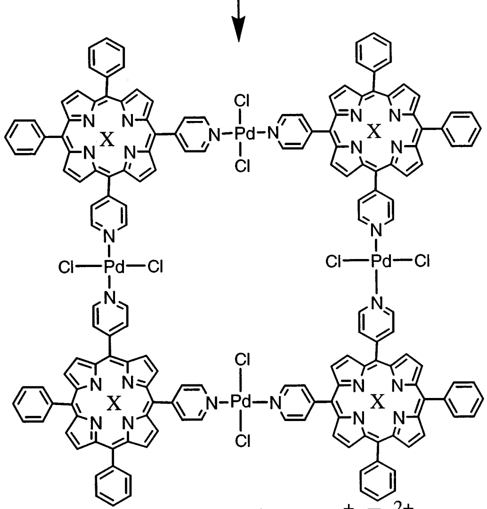

64 X = $2H^+$, Zn^{2+}

Scheme 31.

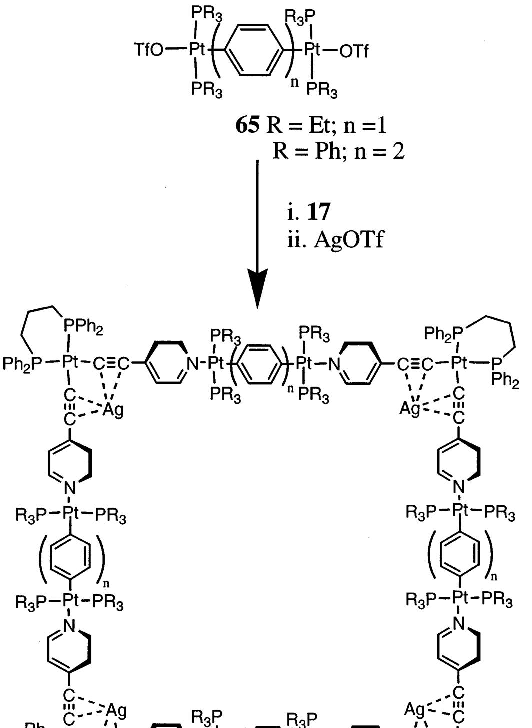

65 R = Et; n =1
R = Ph; n = 2

i. **17**
ii. AgOTf

66

Scheme 32.

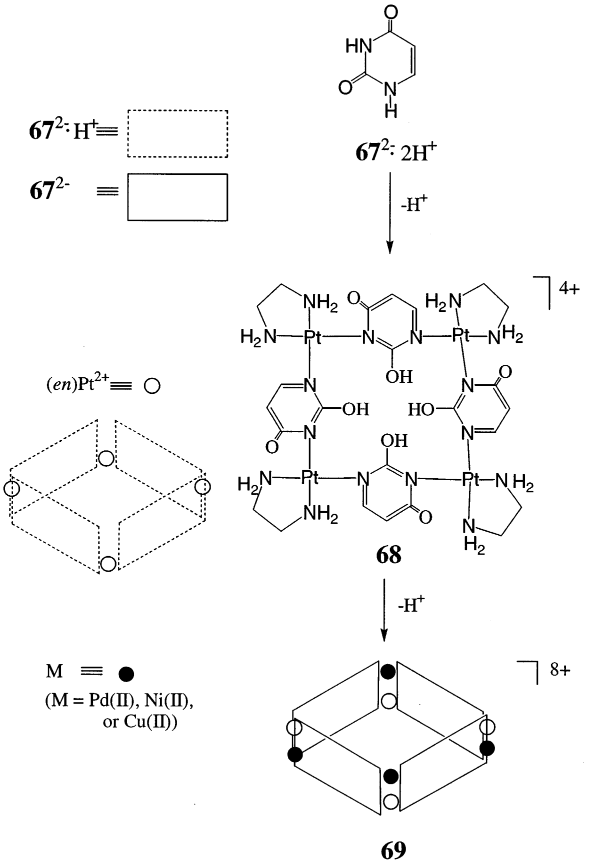

Scheme 33.

binding demands of both the metals and the ligands. Like $A_4^{3a}A_6^{2d}$ adamantanoids and tetrahedra (Section 3.2.4.3) and $A_4^{3a}L_6^{2d}$ tetrahedra (Section 3.2.4.4), $A_4^{3a}A_4^{3d}$ tetrahedra also display *T*-molecular symmetry. One other example of such a box is known [88c].

3.2.4.6. $A_4^{2a}A_2^{4a}A_8^{1d1d}$ assemblies. When $NiCl_2$ is treated with amidinothiourea **77**, the $A_4^{2a}A_2^{4a}A_8^{1d1d}$ rectangular box **78** is self-assembled (Scheme 39) [89]. The formation of this box may be anion controlled as it contained an encapsulated chloride ion in the solid state. Similar boxes were not formed when nitrate, acetate or perchlorate were used as anions; oligomeric products were generated in those cases. The oligomers spontaneously reverted to the rectangular box when potassium chloride was added, however.

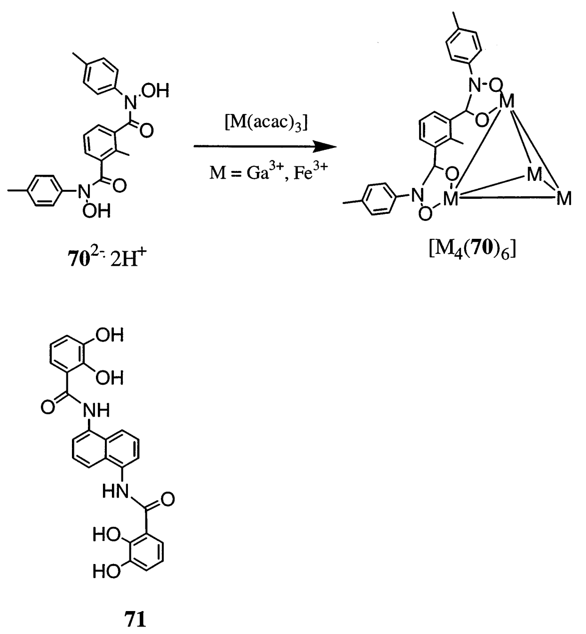

Scheme 34.

3.2.4.7. $A_4^{2a}A_1^{8d}$ assemblies. The rectangular box **69** (Scheme 33) is an example of an ensemble having an $A_4^{2a}A_1^{8d}$ descriptor [75]. Polyhedra of this type have been prepared using various nucleobases, including uracil (**67**$^{2-}\cdot 2H^+$), 1-methylcytosin and 2-aminopyridine as linking units. All are prepared via kinetically stable A^{8d} square intermediates like **68**, which give the rectangular boxes upon deprotonation and addition of labile divalent cations like Pd^{II}, Ni^{II}, and Cu^{II}. The addition of cyanide regenerates the original tetranuclear species **68** almost immediately, indicating the lability of the new linkages. The intermediate **68** remains intact even after stirring for extended periods in the presence of cyanide, indicating its kinetically stable character.

3.2.4.8. $A_4^{4a}L_4^{4d}$ assemblies. An unusual case of a rectangular molecular box having two preformed A^{4a} metal ion units in each corner has been obtained in the reaction of the dirhodium(II) compound **79** with ben-

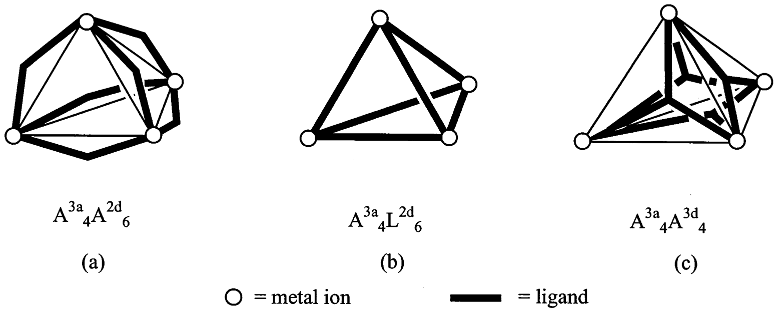

Fig. 6. Schematic depiction of A_4^{3a} clusters showing (a) an edge filled adamantanoid, (b) an edge filled tetrahedron, and (c) a face filled tetrahedron.

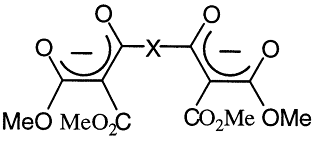

72a X = single bond
72b X = 1,4-Ph
72c X = 4,4′-biphenyl

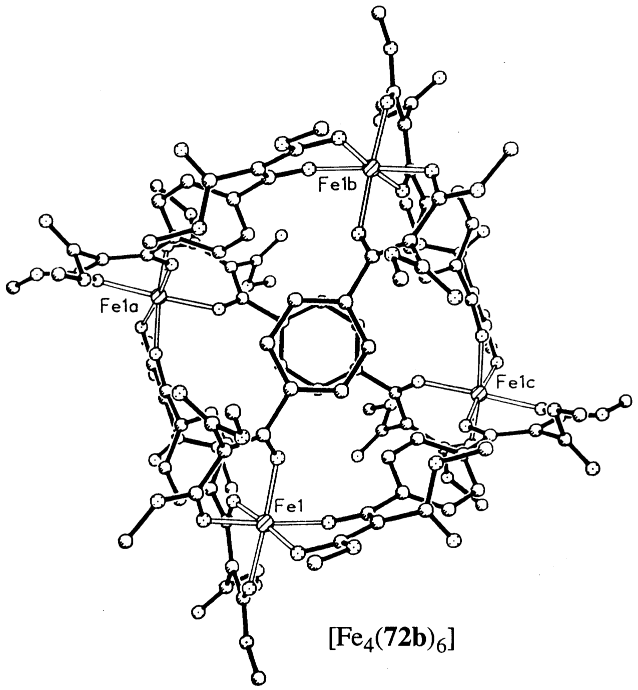

$[Fe_4(\mathbf{72b})_6]$

Fig. 7. ORTEP representation of the neutral tetranuclear adamantanoid box formed in the reaction of Fe(III) with the depronated bis(acetoacetate) **72b**. The central cavity in this molecule is hydrophobic and able to host small ions. (Reproduced with permission; Ref. [80]. Copyright 1993 Wiley-VCH.)

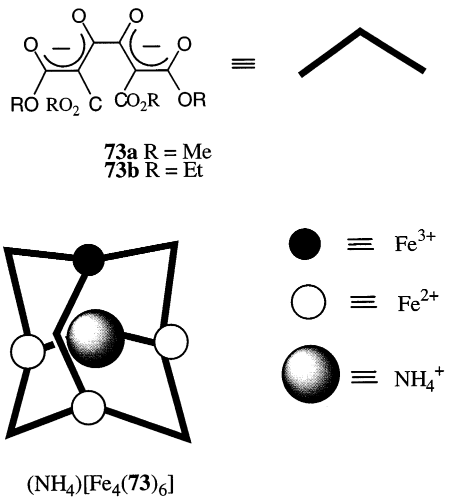

73a R = Me
73b R = Et

$(NH_4)[Fe_4(\mathbf{73})_6]$

Scheme 35.

zene-1,4-dicarboxylic acid (L^{4d} unit) (Scheme 40) [90a]. The resulting $A_4^{4a}L_4^{4d}$ box **80** contained eight Rh^I ions. Similar compounds have been prepared using other co-ligands [90b].

3.2.5. A_6^{na} or L_6^{na} assemblies

Two ways to arrange six metal ions about a central point is in a hexagon (2-D) or an octahedron (3-D). Both of these structures have been reported in A_6^{na} or L_6^{na} assemblies. In an octahedron the metal ions may be bridged in several ways, including on some or all of the edges or faces of the octahedron. As depicted in Fig. 8, $A_6^{2a}A_4^{3d}$ adamantanoids or truncated tetrahedra are formed when four faces are alternately filled about a C_2 axis through two opposing metal ions [91]. An $A_6^{2a}A_6^{3d}$ cylinder is generated when six of the faces are filled leaving the unoccupied faces opposite each other. An $A_6^{2a}A_8^{3d}$ octahedron in which all of the faces are filled by ligands is theoretically possible, but no example has yet been reported. Examples of edge-occupied octahedra have also not been described; such a cluster would have the descriptor $A_6^{4a}L_{12}^{2d}$. An $A_6^{4a}A_{12}^{2d}$ structure is likely to have a truncated octahedron architecture [91b].

Twisting of an octahedron of metal ions leads to a trigonal antiprismatic array about a central point [91]. Clusters of this type are known, although they are generally too distorted to be formed using a single ligand. Instead, the presence of two different ligands—one to link a triangle of metal ions together and the other to link two such triangles into a closed structure—is necessary. Trigonal antiprismatic structures having descriptors such as $A_6^{2a}L_2^{3d}L_3^{2d}$ are consequently known. Such arrangements are common in cylindrical arrays involving metal ions in double-decked trigonal antiprismatic arrangements. They are also related to multi-decked cylinders, including ones having the descriptors $A_9^{2a}L_2^{3d}L_3^{3d}$ (triple-decked) and $A_{12}^{2a}L_3^{4d}L_4^{3d}$ (quadruple-decked).

3.2.5.1. $A_6^{2a}L_6^{2d}$ and $L_6^{2a}A_6^{2d}$ assemblies. The structurally-related $A_6^{2a}L_6^{2d}$ and $L_6^{2a}A_6^{2d}$ hexagons **82** and **83** shown in Schemes 41 and 42, respectively, have been reportedly prepared by interchanging components in the linear and angular building blocks from which these structures were obtained [92]. In the case depicted in Scheme 41, an $A_6^{2a}L_6^{2d}$ hexagon was formed by the reaction of linear 4,4′-bipyridine **39** with the di(platinum(II)) complex **81** which was made angular by the presence of a bis(benzyl)methyl ketone linker. However, when the angular bipyridyl ketone **41c** was treated with the linear di(platinum(II)) complex **65** (R = Ph; $n = 2$), a $L_6^{2a}A_6^{2d}$ hexagonal assembly was obtained (Scheme 42). In both cases the angular units exhibited directing angles of 120°. Twelve individual building blocks were spontaneously and cooperatively assembled to form each hexagon. The structures of the hexagons were deduced

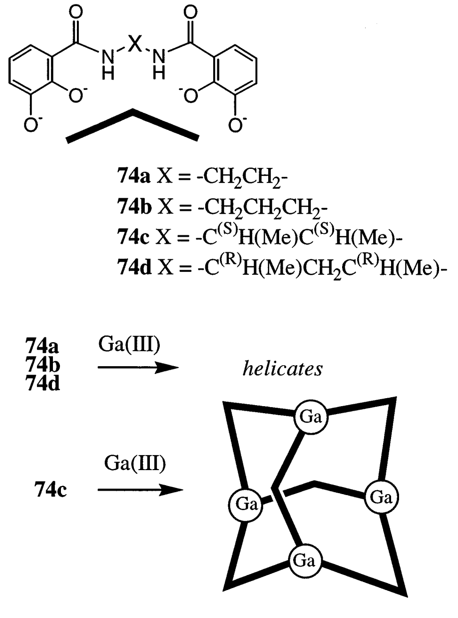

Scheme 36.

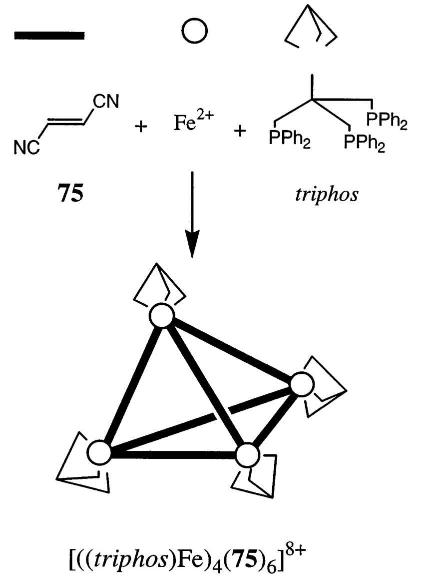

Scheme 37.

from molecular mechanics calculations supported by spectroscopic data.

3.2.5.2. $A_6^{2a}A_4^{3d}$ assemblies. The only way in which six ditopic metals can bind four tritopic ligands is by the formation of an $A_6^{2a}A_4^{3d}$ adamantanoid-like structure, with the ligands in the bridgehead positions and the metals on the connecting vertices. Such structures may be termed hexanuclear adamantanoid boxes although the overall shape of the complex is that of a truncated tetrahedron if the tritopic ligands are planar. $A_6^{2a}A_4^{3d}$ assemblies are the coordinative reverse of $A_4^{3a}A_6^{2d}$ tetrahedron assemblies, with the donor and acceptor units interchanged; both of these cluster types therefore exhibit *T*-symmetry.

The self-assembled hexanuclear $A_6^{2a}A_4^{3d}$ truncated tetrahedra $[((en)Pd)_6(\mathbf{84})_4]^{12+}$ shown in Scheme 43 were obtained by Fujita et al. [93] from six equiv. of $(en)Pd(NO_3)_2$ (**44**) and four equiv. of the 2,4,6-tri-4-pyridyl-1,3,5-triazine derivatives **84**. The overall archi-

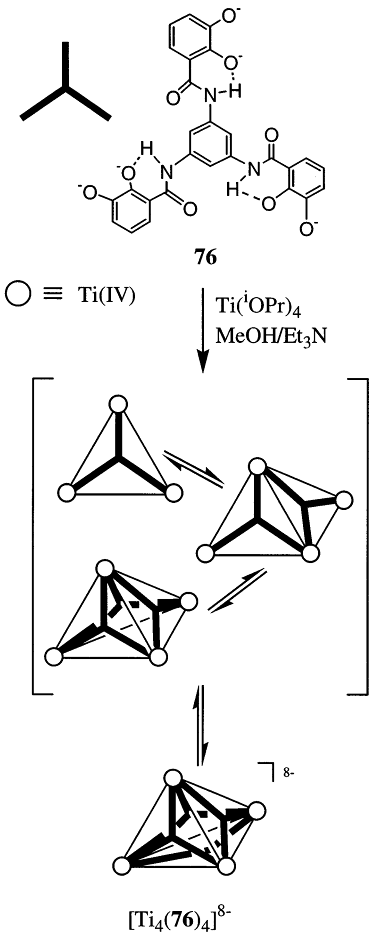

Scheme 38.

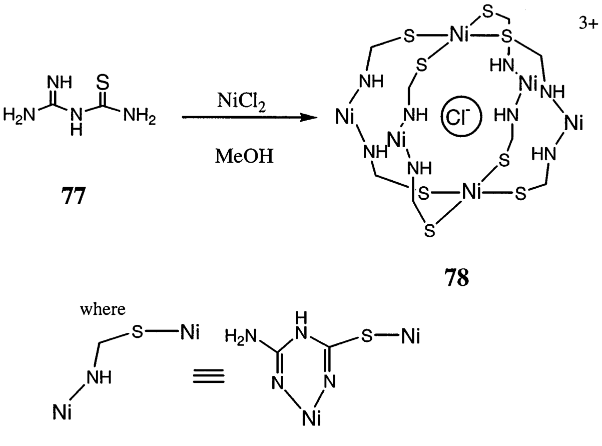

Scheme 39.

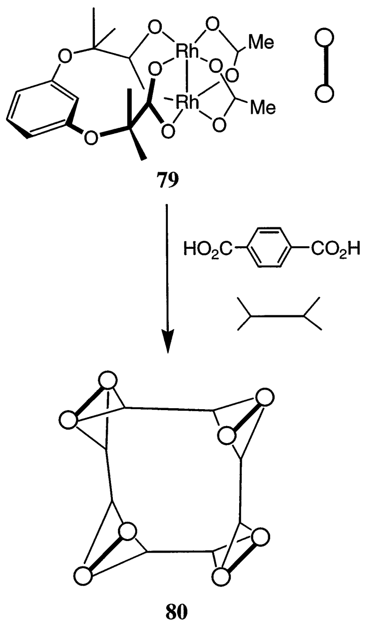

Scheme 40.

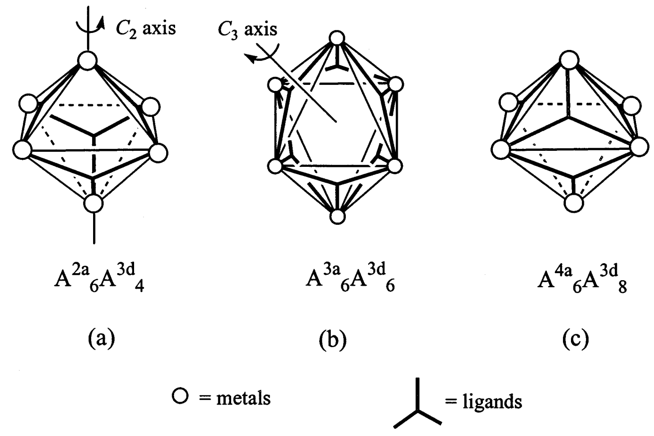

Fig. 8. Schematic depiction of face-bound molecular polyhedra containing six metal ions (open circles) in an octahedral arrangement about a central cavity; (a) hexanuclear adamantanoid or truncated tetrahedron, (b) a type of molecular cylinder, and (c) a molecular octahedron.

tecture of these complexes was revealed by an X-ray crystal structure of the cluster where Ar = single bond. Suitable crystals could only be formed in the presence of 1-adamantane carboxylate, which produced a clathrate complex of sufficient stability. The central nanosized cavity in this molecule contained four guest molecules; this aggregation persisted in aqueous media according to NMR studies. The nanometer-sized scale of the larger derivatives, involving phenylene- or biphenylene-bridged ligands, was confirmed by laser scattering, particle-sizing techniques. 'C-shaped' compounds, such as *cis*-azobenzene and -stilbene derivatives have also been selectively clathrated [94b]. The internal cavity of these truncated tetrahedra have been used as reaction vessels for the selective 'ship-in-a-bottle' formation or stabilisation of novel species [94].

Chiral $A_6^{2a}A_4^{3d}$ truncated tetrahedra $[((R\text{-binap})M)_6(\mathbf{85})_4]^{12+}$ have also been self-assembled using M^{II} (M = Pt, Pd) complexes of *R*-binap as shape-defining corner units and the benzene tri(ethynyl pyridyl) ligand **85** as a connector (Scheme 44) [95]. The structure of this complex, which exhibits *T*-symmetry, was inferred from mass spectrometry and molecular mechanics simulations. The self-assembly proved to be highly pathway specific; i.e. the product architecture was dependent on the order in which the reagents were mixed.

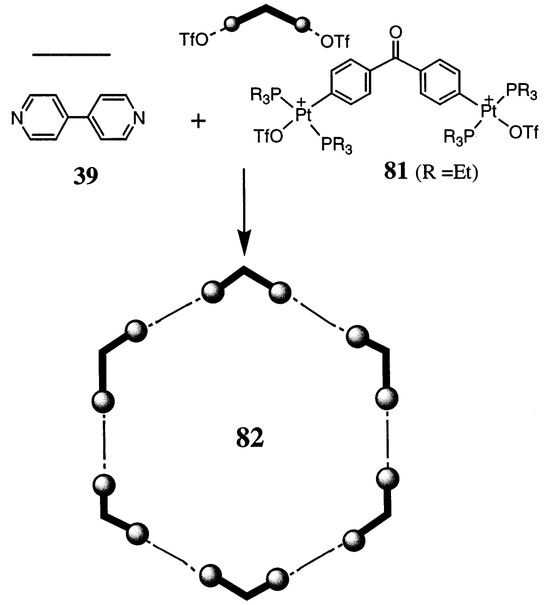

Scheme 41.

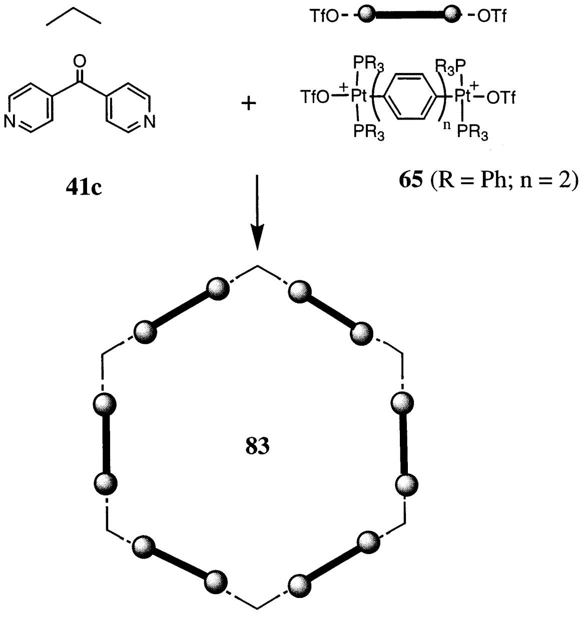

Scheme 42.

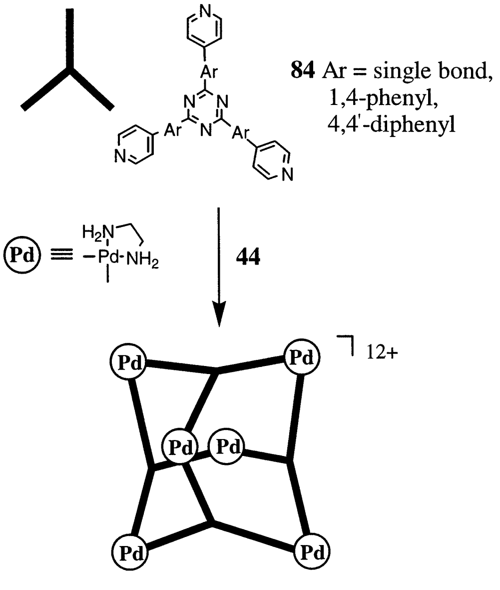

$[((en)Pd)_6(\mathbf{84})_4]^{12+}$

Scheme 43.

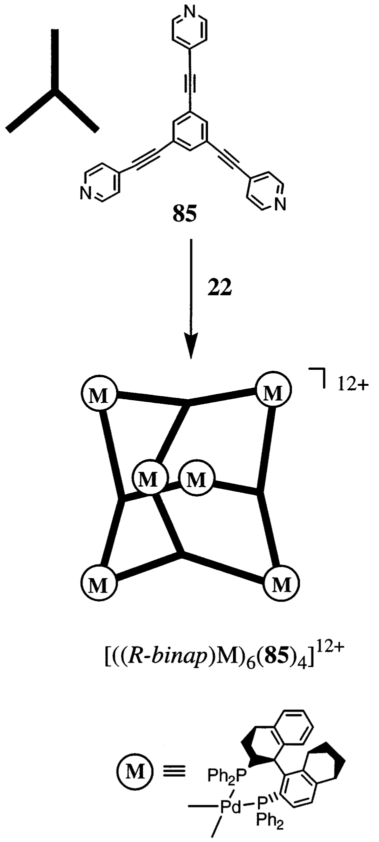

$[((R\text{-}binap)M)_6(\mathbf{85})_4]^{12+}$

Scheme 44.

Truncated tetrahedra/adamantanoids have been prepared using other planar [96,97] and non-planar [98] tridentate linking ligands. A remarkable and unique truncated tetrahedron has also been reported in which each bridgehead position is filled by a Mo_2^{4+} unit [99].

3.2.5.3. $A_6^{2a}A_6^{3d}$ assemblies. The first $A_6^{2a}A_6^{3d}$ assembly has recently been reported by Saalfrank and Raymond [100]. The reaction of $Ga(acac)_3$ (acac = acetylacetonate) with the tritopic ligand **86** resulted in the formation of the molecular cylinder $[Ga_6(\mathbf{86})_6]$ (Scheme 45). While depicted as an octahedron, the arrangement of metal ions in this molecule, in fact, lies neatly between an octahedral and a trigonal antiprismatic structure. It is, moreover, compressed along the pseudo C_3 axis which runs through the two open faces; these are consequently larger than the occupied faces. The molecule has an idealised D_3 molecular symmetry and was obtained as a racemic mixture of homochiral hexanuclear clusters in the solid state.

3.2.5.4. $A_6^{2a}A_2^{3d3d}$ assemblies. The $A_6^{2a}A_2^{3d3d}$ hexagonal box $[(CuPPh_3)_6(\mathbf{87})_2]$ has been obtained in the reaction of trithiocyanuric acid, $\mathbf{87}^{3-}\cdot 3H^+$, with three equiv. of $CuCl(PPh_3)_3$ in the presence of triethylamine (Fig. 9) [101]. In this species, each Cu^I ion has a distorted three-coordinate geometry. The parallel triazine rings are 3.07 Å apart. At room temperature in the solid state, the complex luminescences at 562 nm with an excited state lifetime of 0.59 μs.

3.2.5.5. $A_{3n}^{2a}L_n^{3d}L_3^{nd}$ assemblies (n = 2, 3, 4). $A_6^{2a}L_2^{3d}L_3^{2d}$ double-decker, $A_9^{2a}L_3^{3d}L_3^{3d}$ triple-decker, and $A_{12}^{2a}L_3^{4d}L_4^{3d}$ quadruple-decker cylinders like **90**, **91**, and **92**, respectively (Figs. 10 and 11), have the following relationships in common. They all comprise metal ions in single- or

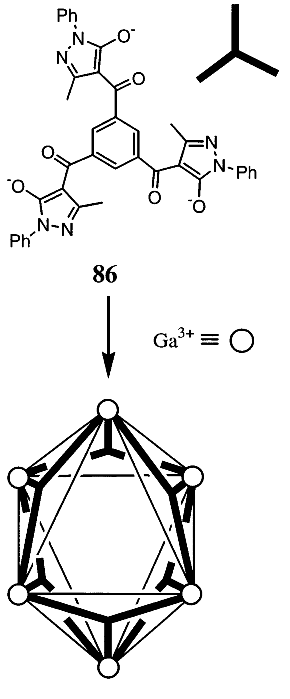

$[Ga_6(\mathbf{86})_6]$

Scheme 45.

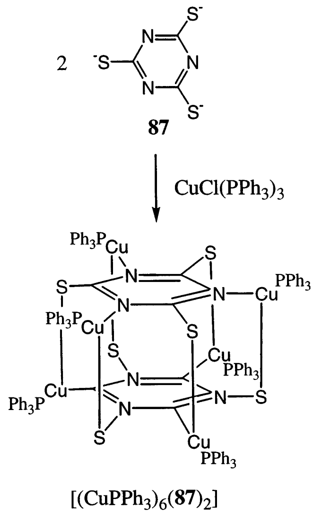

Fig. 9. Formation of a cyclophane/hexagonal box generated by the self assembly of trithiocyanuric acid with $CuCl(PPh_3)_3$ in the presence of Et_3N.

multiply-decked trigonal prismatic arrangements and can therefore have only $3n$ acceptor units present (n = 2, 3, 4). They additionally always incorporate two different donor building blocks, a flat, cyclic ligand having binding sites about its centre (L^{3d}), and a linear ligand having n binding sites down its length (L^{nD}). Stoichiometry considerations lead to the general descriptor $A_{3n}^{2a}L_n^{3d}L_3^{nd}$ ($n = 2$, 3, 4).

The reaction of the cyclic hexaphenylhexaazatriphenylene ligand **88** (L^{3d} unit) and the linear bis(-bipyridine) ligand **89a** (L^{2d} unit) with $[Cu(CH_3CN)_4]$-(BF_4) ($Cu^I = A^{2a}$ unit) in a stoichiometric ratio of 2:3:6 resulted in the formation of the $A_6^{2a}L_2^{3d}L_3^{2d}$ cylinder **90** (Fig. 10) [102]. The cylinder—which is a thermodynamic product—had to be prepared in the absence of halogen or aromatic counter-ions which inhibited the self-assembly. An X-ray crystal structure determination revealed **90** to be twisted about its central compartment (cavity) in the solid state, shortening its length along the cylindrical axis [103]. The reaction of the ligands with silver(I) triflate produced an analogous cylinder which was not twisted in the solid state [104].

Triple-decker ($A_9^{2a}L_3^{3d}L_3^{3d}$) and quadruple-decker ($A_{12}^{2a}L_3^{4d}L_4^{3d}$) cylinders, **91** and **92**, have similarly been prepared by combining **88** (L^{3d} unit) with Cu^I or Ag^I (A^{2a} unit), and ligands **89b** (L^{3d} unit) or **89c** (L^{4d} unit), respectively (Fig. 11) [105]. The resulting cylinders were highly stable, remaining associated even at concentrations as low as 10^{-4} mol dm^{-3}. NMR studies showed that the cylinders were symmetrical in solution and that their cavities contained anions which were able to move in and out at room temperature. As the cylinders are twisted into triple-helical, cage-like structures in the solid state, intramolecular ‘breathing’ of the complexes in solution, by successive winding and unwinding of the helix, was thought to momentarily open the faces, allowing movement into and out of the cavities.

Several other cylindrical complexes having a similar descriptor, but widely differing physical length have been prepared [104]. While cylinder **90** is 20 Å long, analogous double-decker cylinders of up to 33 Å in length were obtained by using the axial ligands **93a**–**e** (Chart 6). The size of the compartments in these cases was enlarged by the use of longer linkers between the binding sites of the axial ligands.

The use of octahedrally-disposed metal ions may also lead to cylinders. The reaction of Pb^{II} with a tris(2-pyrimidyl)-triazine **94** and bis- or tris(terpyridine) lig-

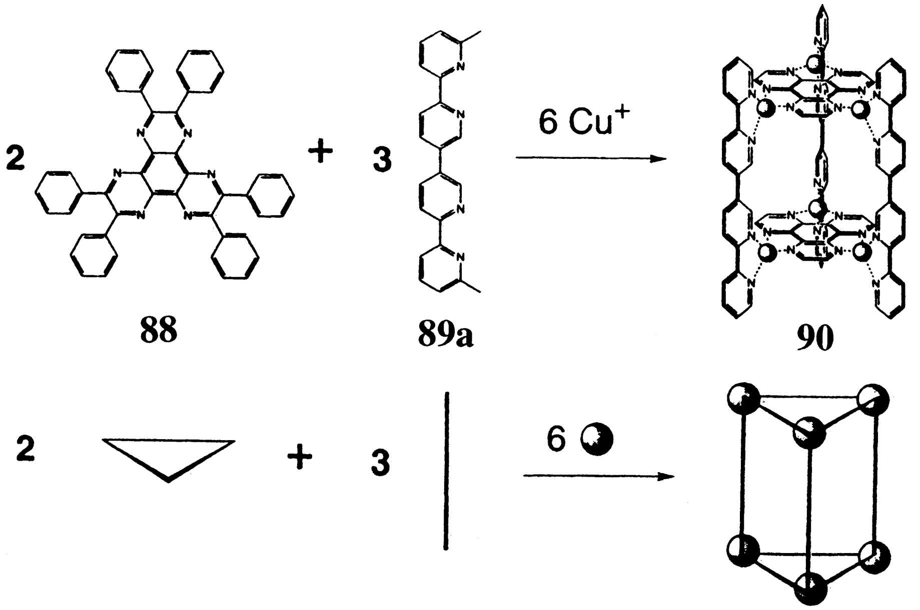

Fig. 10. Formation of a molecular cylinder. (Reproduced with permission; Ref. [102] Copyright 1996 the American Chemical Society.)

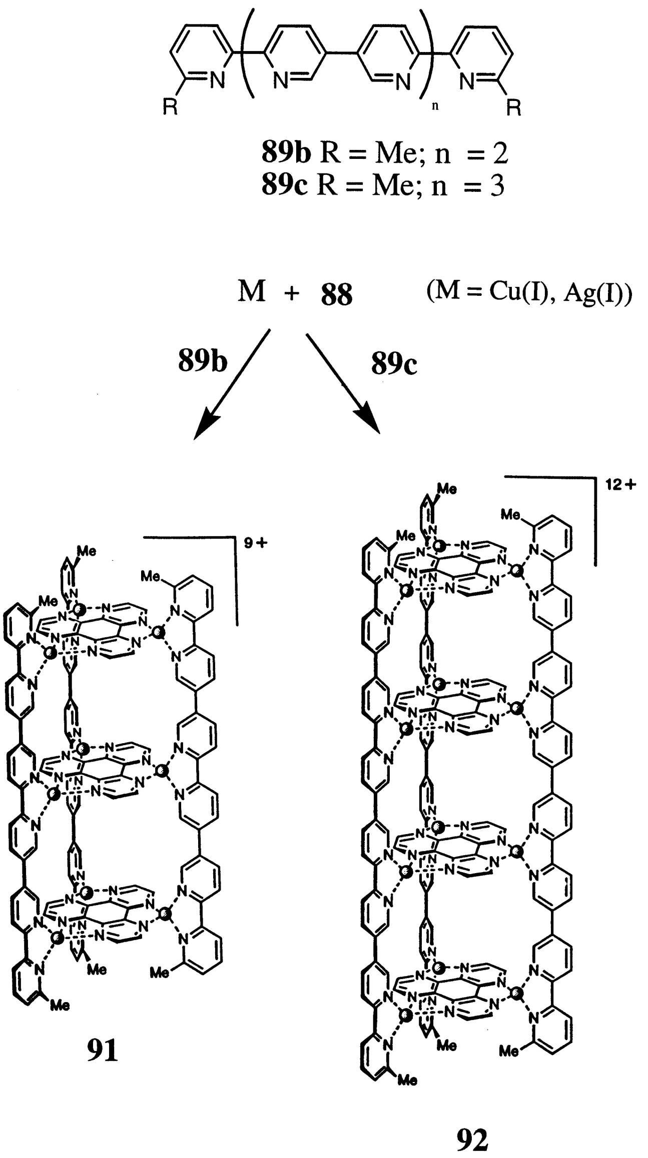

Fig. 11. The formation of triple-decker and quadruple-decker cylinders. The shaded circles represent Cu(I) or Ag(I) ions. (Reproduced with permission; Ref. [105a]. Copyright 1999 Wiley-VCH.)

ands **95** (Chart 6) resulted in the formation of an $A_6^{2a}L_2^{3d}L_3^{2d}$ double-decker and an $A_9^{2a}L_3^{3d}L_3^{3d}$ triple-decker cylinder, respectively [106]. In the solid state, the Pb^{II} ions in the double-decker complex were found to also coordinate the oxygens of two triflate anions.

3.2.5.6. Other A_6^{na} and L_6^{na} assemblies. The reaction of the tripodal ligand **96** with sodium hydride in the presence of $FeCl_3$ led to the [12]metallacrown-6, $[Na \subset Fe_6\{N(CH_2CH_2O)_3\}_6]^+$ **97a** (Scheme 46) [52]. This material, which encapsulates a sodium ion in its central cavity, can be considered a molecular hexagon. Larger metallacrowns are formed in the presence of larger cations, such as Cs^+ (e.g. **97b**; see Section 3.2.6.1). The use of lithium hydride instead of sodium hydride led to small amounts of the corresponding tetranuclear [8]metallacrown-4, $[Li \subset Fe_4\{N(CH_2CH_2O)_3\}_4]^+$, in addition to $[Li \subset Fe_6\{N(CH_2CH_2O)_3\}_6]^+$, which forms the major product. In the presence of CaH_2, the hexanuclear hexagon $[Fe_6\{N(CH_2CH_2O)_3\}_6]^+$ was formed; the central cavity in this molecule was unoccupied.

While each ligand in **97a** forms four coordinate bonds, two of these do not involve linkages essential to

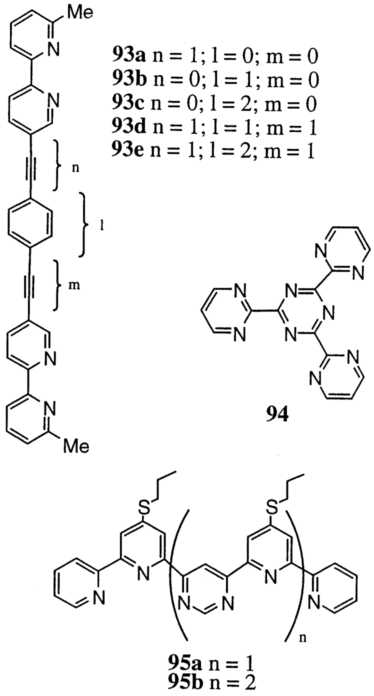

Chart 6.

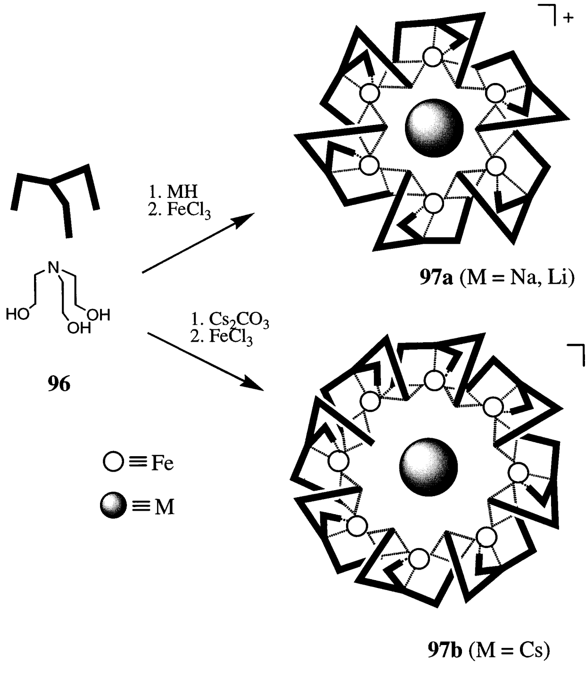

Scheme 46.

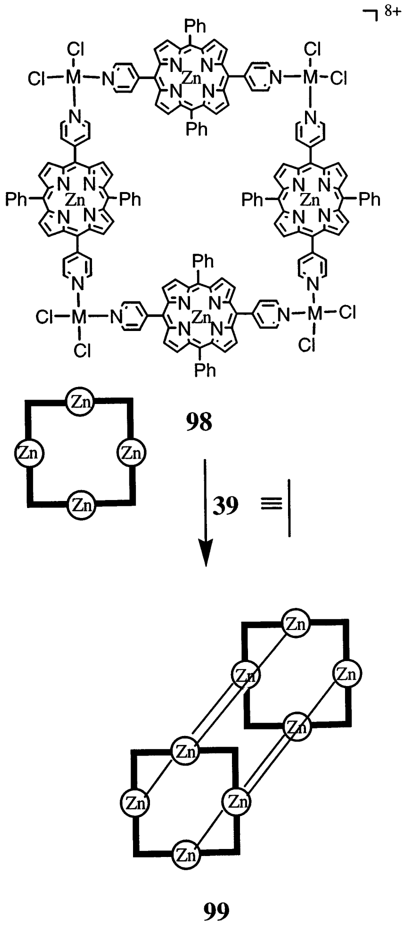

Scheme 47.

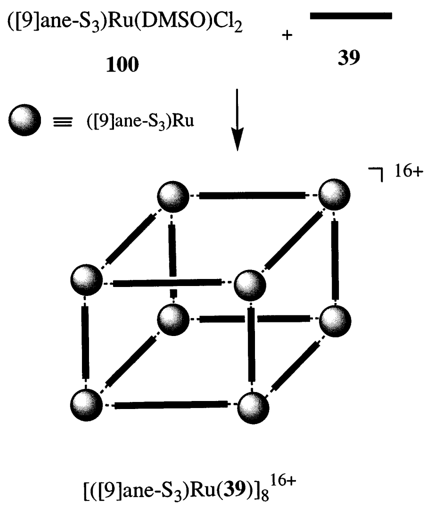

Scheme 48.

the securing of the structure. The remaining two bonds form separate linkages which bridge adjacent metal ions. Each of the ligand building blocks therefore have the descriptor A^{2d2d}. The metal ions form six coordinate bonds each, two of which are not part of the hexagonal scaffold. The remaining four binding sites can be considered identical as far as the metal ions are concerned. This assembly is therefore best described as an $A_6^{4a}A_6^{2d2d}$ hexagon.

3.2.6. A_8^{na} or L_8^{na} assemblies

Structures incorporating eight corners include octagons (2-D) and cubes or rectangular boxes (3-D). Examples of these structures have been self-assembled. Hexagons having the descriptor $A_8^{4a}A_8^{2d2d}$ have been reported, as have symmetrical cubes having the descriptor $A_8^{3a}L_{12}^{2d}$. A rectangular box involving three building blocks is also known; it has the descriptor $L_8^{2a}A_8^{1a2d}A_4^{2d}$. While several other descriptors are possible for the formation of polygons and polyhedra containing eight acceptor units, no other examples have been reported.

3.2.6.1. $A_8^{4a}A_8^{2d2d}$ assemblies. The reaction of **96** with $FeCl_3$ in the presence of Cs_2CO_3 leads to the [16]metallocrown-8, **97b**, depicted in Scheme 46 [52]. This compound encapsulates a caesium ion in its central cavity and can be considered an $A_8^{4a}A_8^{2d2d}$ molecular octagon for the reasons given in Section 3.2.5.6. The formation of **97a**–**b** requires the spontaneous and correct assembly of 13 or 17 components, respectively. This system is a neat example of the effect of metal ions in the formation of metallocycles. Anions have been used to similar effect in the formation of circular helicates [107].

3.2.6.2. $L_8^{2a}A_8^{1a2d}A_4^{2d}$ assemblies. According to ^1H-NMR evidence, treatment of the coordinatively unsaturated $L_4^{2a}A_4^{1a2d}$ molecular square **98** with 4,4′-bipyridyl **39** produces the $L_8^{2a}A_8^{1a2d}A_4^{2d}$ rectangular box **99** which is secured by axial coordination of pyridyl *N*-donor atoms to the porphyrin Zn^{II} ions (Scheme 47) [72]. In this process, the four A^{1a2d} zincated porphyrin units became coordinatively saturated.

3.2.6.3. $A_8^{3a}L_{12}^{2d}$ assemblies. The reaction over several weeks of [([9]ane-S_3)Ru(DMSO)Cl_2] **100** with 4,4′-biypyridine **39** in an 8:12 molar ratio, resulted in the formation of the $A_8^{3a}L_{12}^{2d}$ cube $[([9]\text{ane-}S_3)\text{Ru})(\mathbf{39})]_8^{16+}$, which contains eight Ru^{II} corner ions linked by twelve of the bipyridine ligands (Scheme 48) [108]. Structures other than a cube were inconsistent with the crystallographic, mass spectral and NMR data. Interestingly, this box exhibited three oxidation waves in cyclic voltammetry, rather than the one which may have been anticipated; an interaction between the metal ions therefore exists. Interactions of this type raise the possibility of novel molecular devices, such as multiple-state switches or tunable sensors. The host–guest chemistry of such boxes may influence electron and energy transfer processes. One other discrete, but smaller $A_8^{3a}L_{12}^{2d}$ cube has also been reported [109].

3.2.6.4. $A_8^{3a}A_{12}^{2d}$ assemblies. The neutral $A_8^{3a}A_{12}^{2d}$ complex $[Cu_{12}(\mathbf{101})_8]$ (Scheme 49) has been formed by treatment of the deprotonated ligand **101** with $Cu(NO_3)_2$ [110]. Because the resulting complex contains eight three-sided centres (the ligands), it conforms to the topological structure of a truncated cube (as depicted in Scheme 49). However, if the truncation planes are considered to include the Cu(II) ions at their vertices, the structure can also be considered a cuboctahedron (like that depicted in Scheme 50). The void in the centre of this molecule was unoccupied and had a volume of ca. 816 Å^3.

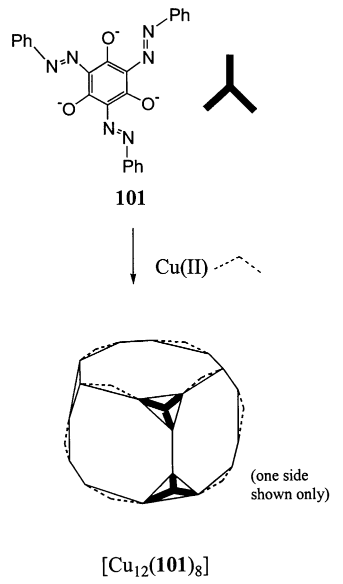

Scheme 49.

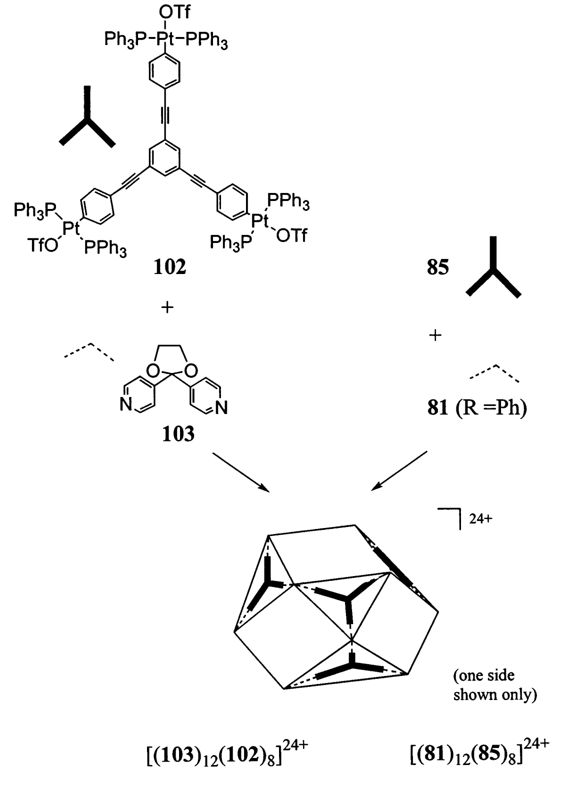

Scheme 50.

Cubic/cuboctahedral $A_8^{3a}A_{12}^{2d}$ compounds of near-identical structure have also been formed in the reaction of 8 equiv. **102** with 12 equiv. **103** and the reaction of **85** with **81** (R = Ph) in similar proportions (Scheme 50) [111]. The resulting cuboctahedral capsules were the first examples of coordination compounds having *O*-symmetry. They were characterised by NMR and mass spectrometry. According to force field simulations, these molecules fill a spheroid of diameter ca. 5 nm.

3.2.7. A_9^{na} or L_9^{na} assemblies

Several triple-decker cylinders having the descriptor $A_9^{2a}L_3^{3d}L_3^{3d}$ have been described in Section 3.2.5.5. To the best of our knowledge no other assemblies containing nine acceptor units are known, although many are theoretically possible.

3.2.8. A_{12}^{na} or L_{12}^{na} assemblies

Titration of the coordinatively unsaturated $L_{12}^{2a}A_1^{1a4d}A_4^{1a3d}A_4^{1a2d}$ square array $[Pd_{12}Cl_{24}(\mathbf{28})_4(\mathbf{104})_4(\mathbf{105})_1]$ (Scheme 51) with 4,4′-bipyridine **39** produces a sandwich of nine bipyridyl ligands between two nonamer zinc–porphyrin arrays [112]. Axial Zn-N(bipyridine) coordination bonds secure this box. While the zinc ions were not coordinated in the original array, they became coordinated in the square box. The L-shaped porphyrin unit, **28**, which was a coordinatively unsaturated A^{1a2d} unit becomes saturated in the process; similar changes occurred for the T-shaped unit **104** and the X-shaped unit **105**. The new assembly therefore has the rather complicated descriptor $L_{12}^{2a}A_1^{1a4d}A_4^{1a3d}A_4^{1a2d}L_9^{2d}$; five different building blocks are self-assembled into a single complex. The nine L^{2d} units describe the linking bipyridine molecules.

Several quadruple-decker $A_{12}^{2a}L_3^{4d}L_4^{3d}$ cylinders have been described in Section 3.2.5.5.

3.2.9. Larger assemblies

3.2.9.1. $A_{18}^{2a}A_6^{6d}$ trigonal bipyramids. The hexahedron $[Pd_{18}(\mathbf{106})_6]^{36+}$ (Scheme 52) has recently been prepared by Fujita and co-workers by combining the C_3-symmetric ligand **106** with (en)Pd$(NO_3)_2$ **44**. The (en)Pd units doubly bridge the triangular faces formed by **106**. The compound has an internal volume of ca. 900 Å^3 but this is closed to all but the smallest of molecules because all of the faces are occupied [113].

3.2.9.2. $A_{20}^{3a}L_{30}^{2d}$ dodecahedra. The correct stoichiometric combination of tri(4′-pyridyl)methanol **107** (directing angles 108°) (Scheme 53) with a linear bidentate unit, such as bis[4,4′-*trans*-Pt$(PR_3)_2$OTf]benzene **65** (directing

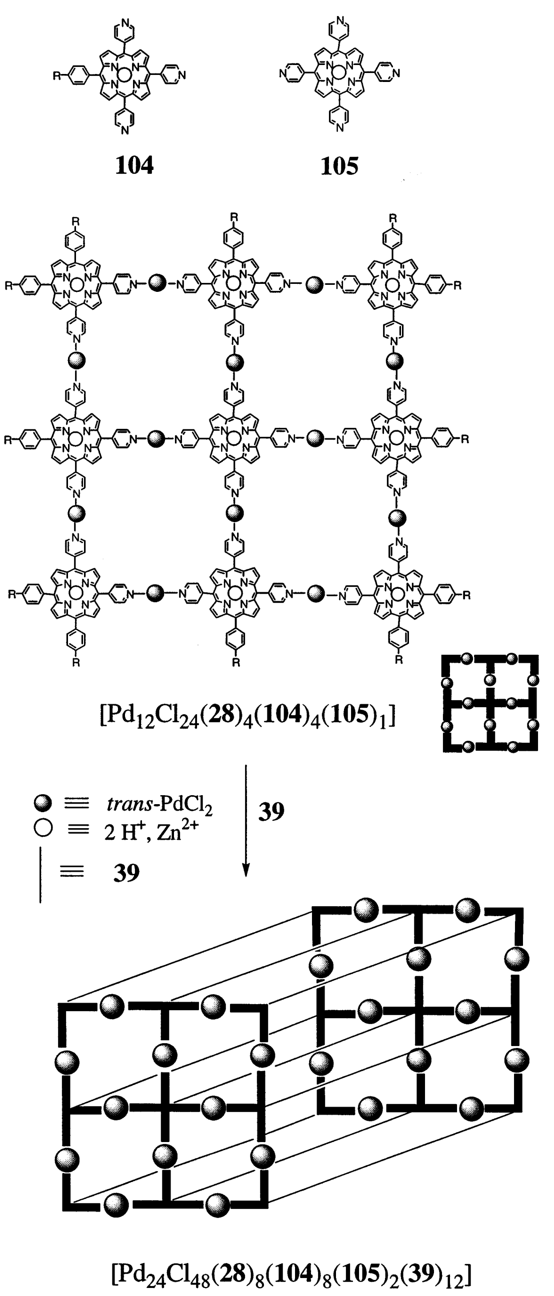

Scheme 51.

angle 180°; R = Et, Ph), produced the first reported $A^{3a}_{20}L^{2d}_{30}$ molecular dodecahedra $[(\mathbf{65})_{30}(\mathbf{107})_{20}]^{60+}$ in quantitative yield [114]. The success of this procedure rested on the rigidity of the building blocks, which were required to correctly transmit the directing effects over nanometer-scale distances. Flexible linkers resulted in the formation of defects which could not self-correct in the thermodynamic equilibrium, so that oligomers were instead obtained. The dodecahedra enclose spheroids of diameter 5–8 nm. Each could be imaged by TEM micrography. The self-assembly of each dodecahedron involved the in-situ formation of 60 coordination bonds between 50 individual molecules in solution.

4. Conclusion

In this work we have catalogued known molecular polygons and polyhedra in terms of their assembly descriptor notation. The descriptors allow known compounds to be readily compared with newly prepared or conceived compounds having self-assembly processes of similar stoichiometry and type. Identical or near-identical self-assembly pathways and common building block types are thereby revealed. The conceptualisation of self-assembly processes and the selection of interacting units for the formation of novel structural architectures is, moreover, facilitated. Useful commonalities and relationships between different polygons and polyhedra,

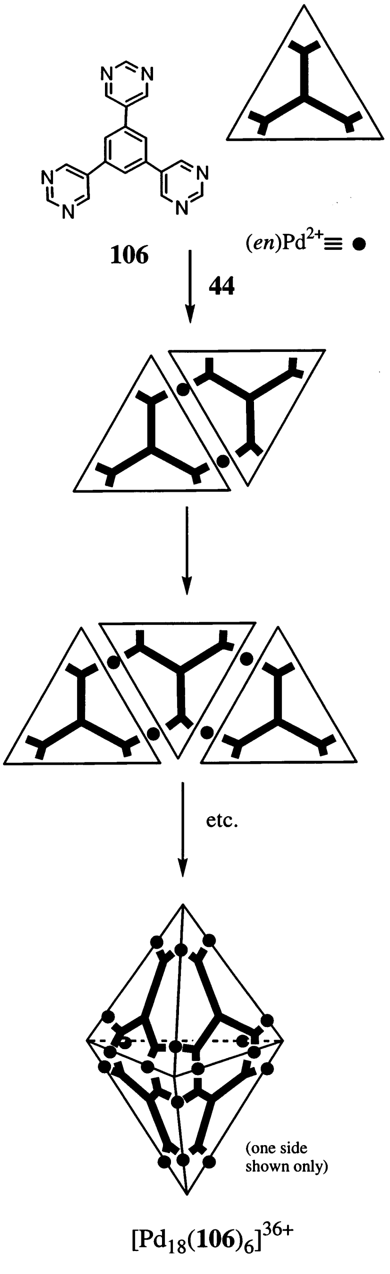

Scheme 52.

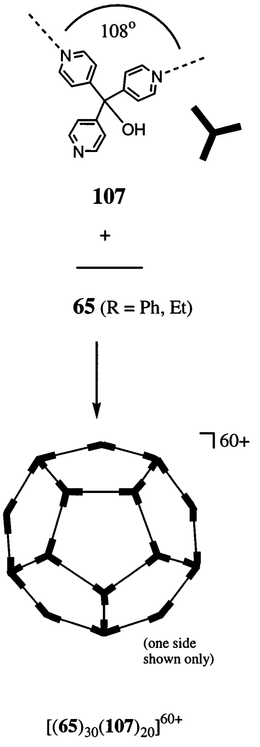

Scheme 53.

and their mode of self-assembly are also more clearly illustrated.

Acknowledgements

T.J.M. acknowledges, with thanks, a travel fellowship provided by the National Research Foundation (South Africa), as well as the kind hospitality of both the Department of Chemistry at the University of Wollongong (Australia) and the CSIRO Division of Molecular Science (Australia).

References

[1] G.F. Swiegers, T.J. Malefetse, Chem. Rev. 100 (2000) 3483.

[2] (a) S. Leininger, B. Olenyuk, P.J. Stang, Chem. Rev. 100 (2000) 853;
(b) D.L. Caulder, K.N. Raymond, Acc. Chem. Res. 32 (1999) 975.

[3] G.F. Swiegers, T.J. Malefetse, Chem. Eur. J. 7 (2000) 3636.

[4] (a) P.J. Stang, B. Olenyuk, Acc. Chem. Res. 30 (1997) 502;
(b) P.J. Stang, Chem. Eur. J. 4 (1998) 19;
(c) B. Olenyuk, A. Fechtenkötter, P.J. Stang, J. Chem. Soc. Dalton Trans. (1998) 1707.

[5] C.A. Hunter, L.D. Sarson, Angew. Chem. Int. Ed. Engl. 33 (1994) 2313.

[6] M. Gardner, A.J. Guerin, C.A. Hunter, U. Michelsen, C. Rotger, New J. Chem. (1999) 309.

[7] (a) S. Rüttimann, G. Bernardinelli, A.F. Williams, Angew. Chem. Int. Ed. Engl. 32 (1993) 392;
(b) R.F. Carina, A.F. Williams, G. Bernardinelli, J. Organometal. Chem. 548 (1997) 45.

[8] X. Chi, A.J. Guerin, R.A. Haycock, C.A. Hunter, L.D. Sarson, J. Chem. Soc. Chem. Commun. (1995) 2567.

[9] (a) J. Wojacczynski, L. Latos-Grazynski, M.M. Olmstead, A.L. Balch, Inorg. Chem. 36 (1997) 4548;
(b) J. Wojacczynski, L. Latos-Grazynski, Inorg. Chem. 34 (1995) 1044;
(c) J. Wojacczynski, L. Latos-Grazynski, Inorg. Chem. 35 (1996) 4812;
(d) J. Wojacczynski, L. Latos-Grazynski, Inorg. Chem. 34 (1995) 1054.

[10] K. Yamanari, I. Fukuda, K. Kawamoto, Y. Kushi, A. Fuyuhiro, N. Kubota, T. Fukuo, R. Arakawa, Inorg. Chem. 37 (1998) 5611.

[11] C.A. Hunter, R.K. Hyde, Angew. Chem. Int. Ed. Engl. 36 (1996) 1936.

[12] E. Alessio, M. Macchi, S.L. Heath, L.G. Marzilli, Inorg. Chem. 36 (1997) 5614.

[13] K. Funatsu, A. Kimura, T. Imamura, Y. Sasaki, Chem. Lett. (1995) 765.

[14] P.J. Stang, J.A. Whiteford, Res. Chem. Intermed. 22 (1996) 659.

[15] (a) N. Matsumoto, Y. Matoda, T. Matsuo, T. Nakashima, N. Re, F. Dahan, J.-P. Tuchagues, Inorg. Chem. 38 (1999) 1165;
(b) N. Matsumoto, Y. Mizuguchi, G. Mago, S. Eguchi, N. Miyasaka, T. Nakashima, J.-P. Tuchagues, Angew. Chem. Int. Ed. Engl. 36 (1997) 1860.

[16] F. Felluga, P. Tecilla, L. Hillier, C.A. Hunter, G. Licini, P. Scrimin, Chem. Commun. (2000) 1087.

[17] P.J. Stang, J.A. Whiteford, Organometallics 113 (1994) 3776.

[18] J.A. Whiteford, C.V. Lu, P.J. Stang, J. Am. Chem. Soc. 119 (1997) 2524.

[19] P.J. Stang, K. Chen, A.M. Arif, J. Am. Chem. Soc. 117 (1995) 8793.

[20] R. Schneider, M.-W. Hosseini, J.-M. Planeix, A. De Cian, J. Fischer, Chem. Commun. (1998) 1625.

[21] B. Olenyuk, J.A. Whiteford, P.J. Stang, J. Am. Chem. Soc. 118 (1996) 8221.

[22] C. Müller, J.A. Whiteford, P.J. Stang, J. Am. Chem. Soc. 120 (1998) 9827.

[23] J.A. Whiteford, P.J. Stang, S.D. Huang, Inorg. Chem. 37 (1998) 5595.

[24] A.-K. Duhme, S.C. Davies, D.L. Hughes, Inorg. Chem. 37 (1998) 5380.

[25] F.S. McQuillan, C.J. Jones, J.A. McCleverty, Polyhedron 14 (1995) 3157.

[26] T. Habicher, J.-F. Nierengarten, V. Gramlich, F. Diederich, Angew. Chem. Int. Ed. Engl. 37 (1998) 1916.

[27] S.C. Dixit, R. Sharon, R.N. Kapour, Inorg. Chim. Acta 158 (1989) 109.

[28] R. Ziessel, D. Matt, L. Toupet, J. Chem. Soc. Chem. Commun. (1995) 2033.

[29] K. Funatsu, A. Kimura, T. Imamura, Y. Sasaki, Chem. Lett. (1995) 765.

[30] C.M. Drain, J.-M. Lehn, J. Chem. Soc. Chem. Commun. (1994) 2313.

[31] J. Fan, J.A. Whiteford, B. Olenyuk, M.D. Levin, P.J. Stang, E.B. Fleischer, J. Am. Chem. Soc. 121 (1999) 2741.

[32] M. Schmitz, S. Leininger, J. Fan, A.M. Arif, P.J. Stang, Organometallics 18 (1999) 4817.

[33] S.-S. Sun, A.S. Silva, I.M. Brinn, A.J. Lees, Inorg. Chem. 39 (2000) 1344.

[34] M. Fujita, S. Nagao, M. Lida, K. Ogata, K. Ogura, J. Am. Chem. Soc. 155 (1993) 1574.

[35] (a) R.V. Sloane, K.D. Benkstein, S. Belanger, J.T. Hupp, I.A. Guzei, A.L. Rheingold, Coord. Chem. Rev. 171 (1998) 221 and references therein;

(b) R.V. Sloane, D.I. Yoon, R.M. Calhoun, J.T. Hupp, J. Am. Chem. Soc. 117 (1995) 11813.

[36] T. Bark, T. Weyermüller, F. Heirtzler, Chem. Commun. (1998) 1475.

[37] F. Heirtzler, T. Weyermüller, J. Chem. Soc. Dalton Trans. (1997) 3653.

[38] E.C. Constable, E. Schofield, Chem. Commun. (1998) 403.

[39] A.W. Maverick, S.C. Buckingham, Q. Yao, J.R. Bradbury, G.G. Stanley, J. Am. Chem. Soc. 108 (1986) 7430.

[40] A. Schwabacher, J. Lee, H. Lei, J. Am. Chem. Soc. 114 (1992) 7597.

[41] C.M. Hartshorn, P.J. Steel, Inorg. Chem. 35 (1996) 6902.

[42] M. Fujita, J. Yazaki, T. Kuramochi, K. Ogura, Bull. Chem. Soc. Jpn. 66 (1993) 1837.

[43] S. Aoki, M. Shiro, E. Kimura, J. Am. Chem. Soc. 122 (2000) 576.

[44] M.J. Hannon, C.L. Painting, W. Errington, Chem. Commun. (1997) 307.

[45] M.J. Hannon, C.L. Painting, W. Errington, Chem. Commun. (1997) 1805.

[46] S.-W. Lai, M.C.-W. Chan, S.-M. Peng, C.-M. Che, Angew. Chem. Int. Ed. Engl. 38 (1999) 669.

[47] (a) D.P. Smith, E. Baralt, B. Morales, M.M. Olmstead, M.F. Maestre, R.H. Fish, J. Am. Chem. Soc. 114 (1992) 10647;
(b) H. Cheng, M.M. Olmstead, D.P. Smith, M.F. Maestre, R.H. Fish, Angew. Chem. Int. Ed. Engl. 34 (1995) 1515.

[48] M. Fujita, M. Aoyagi, K. Ogura, Inorg. Chim. Acta 246 (1996) 53.

[49] S. Leininger, M. Schmitz, P.J. Stang, Organic Lett. 1 (1999) 1921.

[50] X. Yang, C.B. Knobler, M.F. Hawthorne, Angew. Chem. Int. Ed. Engl. 103 (1991) 1519.

[51] R.N. Grimes, Angew. Chem. Int. Ed. Engl. 32 (1993) 1289 and references therein.

[52] R.W. Saalfrank, I. Bernt, E. Uller, F. Hampel, Angew. Chem. Int. Ed. Engl. 36 (1997) 2482.

[53] J. Padilla, D. Gatteschi, P. Chaudhuri, Inorg. Chim. Acta 260 (1997) 217.

[54] A. Thompson, S.J. Rettig, D. Dolphin, Chem. Commun. (1999) 631.

[55] (a) R.-D. Schnebeck, L. Randaccio, E. Zangrando, B. Lippert, Angew. Chem. Int. Ed. Engl. 37 (1998) 119;
(b) A.T. Baker, J.K. Crass, M. Maniska, D.C. Craig, Inorg. Chim. Acta 230 (1995) 225.

[56] (a) M. Fujita, O. Sasaki, T. Mitsuhashi, T. Fujita, J. Yakazi, K. Yamaguchi, K. Ogura, J. Chem. Soc. Chem. Commun. (1996) 1535;
(b) M. Fujita, J. Yakazi, K. Ogura, J. Am. Chem. Soc. 112 (1990) 5645.

[57] S.-S. Sun, A.J. Lees, Inorg. Chem. 38 (1999) 4181.

[58] P.N.W. Baxter, J.-M. Lehn, K. Rissanen, Chem. Commun. (1997) 1323.

[59] S.B. Lee, S. Hwang, D.S. Chung, H. Yun, J.-I. Hong, Tetrahedron Lett. 39 (1998) 873.

[60] F.M. Romero, R. Ziessel, A. Dupont-Gervais, A. Van Dorsselaer, Chem. Commun. (1996) 551.

[61] J.R. Hall, S.J. Loeb, G.K.H. Shimizu, G.P.A. Yap, Angew. Chem. Int. Ed. Engl. 37 (1998) 121.

[62] M. Fujita, S. Nagao, K. Ogura, J. Am. Chem. Soc. 117 (1995) 1649.

[63] (a) P.M. van Calcar, M.M. Olmstead, A.L. Balch, Chem. Commun. (1996) 2597;
(b) X. Sun, D.W. Johnson, D.L. Caulder, R.E. Powers, K.N. Raymond, E.H. Wong, Angew. Chem. Int. Ed. Engl. 38 (1999) 1303.

[64] E. Leize, A. Van Dorsselaer, R. Krämer, J.-M. Lehn, J. Chem. Soc. Chem. Commun. (1993) 990.

[65] P.J. Stang, D.H. Cao, S. Saito, A.M. Arif, J. Am. Chem. Soc. 117 (1995) 6273.

[66] P.J. Stang, B. Olenyuk, Angew. Chem. Int. Ed. Engl. 35 (1996) 732.

[67] P.J. Stang, D.H. Cao, K. Chen, G.M. Gray, D.C. Muddiman, R.D. Smith, J. Am. Chem. Soc. 119 (1997) 5163.

[68] P.J. Stang, B. Olenyuk, J. Fan, A.M. Arif, Organometallics 15 (1996) 904.

[69] P.J. Stang, J. Fan, B. Olenyuk, Chem. Commun. (1997) 1453.

[70] (a) S.M. Woessner, J.B. Helms, Y. Shen, B.P. Sullivan, Inorg. Chem. 37 (1998) 5406;
(b) K.D. Benkstein, J.T. Hupp, C.L. Stern, Inorg. Chem. 37 (1998) 5404;
(c) S.M. Woessner, J.B. Helms, J.F. Houlis, B.P. Sullivan, Inorg. Chem. 38 (1999) 4380.

[71] R.V. Sloane, J.T. Hupp, C.L. Stern, T.E. Albrecht-Schmitt, Inorg. Chem. 35 (1996) 4096.

[72] C.-Y. Duan, Z.-H. Liu, X.-Z. You, F. Xue, T.C.W. Mak, Chem. Commun. (1997) 381.

[73] T. Kajiwara, T. Ito, J. Chem. Soc. Chem. Commun. (1994) 1773.

[74] J. Manna, C.J. Kuehl, J.A. Whitford, P.J. Stang, D.C. Muddiman, C.D. Hofstadler, R.D. Smith, J. Am. Chem. Soc. 119 (1997) 11611.

[75] (a) H. Rauter, E.C. Hillgeris, A. Erleben, B. Lippert, J. Am. Chem. Soc. 116 (1994) 616;
(b) H. Rauter, I. Mutikainen, M. Blomberg, C.J.L. Lock, P. Amo-Ochoa, E. Freisinger, L. Randaccio, E. Zangrando, E. Chiarparin, B. Lippert, Angew. Chem. Int. Ed. Engl. 36 (1997) 1296 and references therein.

[76] D.L. Caulder, K.N. Raymond, J. Chem. Soc. Dalton Trans. (1999) 1185 and references therein.

[77] T. Beissel, R.E. Powers, K.N. Raymond, Angew. Chem. Int. Ed. Engl. 35 (1996) 1084.

[78] D.L. Caulder, R.E. Powers, T.N. Parac, K.N. Raymond, Angew. Chem. Int. Ed. Engl. 37 (1998) 1840.

[79] T.N. Parac, D.L. Caulder, K.N. Raymond, J. Am. Chem. Soc. 120 (1998) 8003.

[80] R.W. Saalfrank, B. Hörner, D. Stalke, J. Salbeck, Angew. Chem. Int. Ed. Engl. 32 (1993) 1179.

[81] R.W. Saalfrank, A. Stark, K. Peters, H. Von Schnering, Angew. Chem. Int. Ed. Engl. 27 (1988) 851.

[82] R.W. Saalfrank, A. Stark, M. Bremer, H.-U. Hummel, Angew. Chem. Int. Ed. Engl. 29 (1990) 311.

[83] R.W. Saalfrank, R. Burak, A. Breit, D. Stalke, R. Herbst-Irmer, J. Daub, M. Porsche, E. Bill, M. Muther, A.X. Trautwein, Angew. Chem. Int. Ed. Engl. 33 (1994) 1621.

[84] R.W. Saalfrank, R. Burak, S. Reihs, N. Löw, F. Hampel, H.-D. Stachel, J. Lentmaier, K. Peters, E.-M. Peters, H.G. Von Schnering, Angew. Chem. Int. Ed. Engl. 34 (1995) 993.

[85] E.J. Enemark, T.D.P. Stack, Angew. Chem. Int. Ed. Engl. 37 (1998) 932.

[86] R.L. Paul, S.M. Couchman, J.C. Jeffrey, J.A. McCleverty, Z.R. Reeves, M.D. Ward, J. Chem. Soc. Dalton Trans. (2000) 845.

[87] S. Mann, G. Huttner, L. Zsolnai, K. Heinze, Angew. Chem. Int. Ed. Engl. 35 (1996) 2808.

[88] (a) C. Brückner, R.E. Powers, K.N. Raymond, Angew. Chem. Int. Ed. Engl. 37 (1998) 1837;
(b) S. König, C. Brückner, K.N. Raymond, J.A. Leary, J. Am. Mass Spectrom. 9 (1998) 1099;
(c) A.J. Amoroso, J.C. Jeffrey, P.L. Jones, J.A. McCleverty, P. Thornton, M.D. Ward, Angew. Chem. Int. Ed. Engl. 34 (1995) 1443.

[89] R. Vilar, M.P. Mingos, A.J.P. White, D.J. Williams, Angew. Chem. Int. Ed. Engl. 37 (1998) 1258.

[90] (a) R.P. Bonar-Law, T.D. McGrath, N. Singh, J.F. Bickley, A. Steiner, Chem. Commun. (1999) 2457;

(b) S.L. Schiavo, G. Pocsfalvi, S. Serroni, P. Cardiano, P. Piraino, Eur. J. Inorg. Chem. (2000) 1371.
[91] (a) S. Leininger, J. Fan, M. Schmitz, P.J. Stang, Proc. Natl. Acad. Sci. USA 97 (2000) 1380;
(b) L.R. MacGillivray, J.L. Atwood, Angew. Chem. Int. Ed. Engl. 33 (1999) 1019.
[92] P.J. Stang, N.E. Persky, J. Manna, J. Am. Chem. Soc. 119 (1997) 4777.
[93] M. Fujita, D. Oguro, M. Miyazawa, H. Oka, K. Yamaguchi, K. Ogura, Nature 378 (1995) 469.
[94] (a) M. Yoshizawa, T. Kusukawa, M. Fujita, K. Yamaguchi, J. Am. Chem. Soc. 122 (2000) 6311;
(b) T. Kusukawa, M. Fujita, J. Am. Chem. Soc. 121 (1999) 1397.
[95] P.J. Stang, B. Olenyuk, D.C. Muddiman, R.D. Smith, Organometallics 16 (1997) 3094.
[96] M. Fujita, S.-Y. Yu, T. Kusukawa, H. Funaki, K. Ogura, K. Yamaguchi, Angew. Chem. Int. Ed. Engl. 37 (1998) 2082.
[97] C.M. Hartshorn, P.J. Steel, Chem. Commun. (1997) 541.
[98] S.L. James, D.L.P. Mingos, A.J.P. White, D.J. Williams, Chem. Commun. (1998) 2323.
[99] F.A. Cotton, L.M. Daniels, C.A. Murillo, Chem. Commun. (1999) 841.
[100] D.W. Johnson, J. Xu, R.W. Saalfrank, K.N. Raymond, Angew. Chem. Int. Ed. Engl. 38 (1999) 2882.
[101] C.-K. Chan, K.-K. Cheung, C.-M. Che, Chem. Commun. (1996) 227.
[102] A. Marquis-Rigault, A. Dupont-Gervais, P.N.W. Baxter, A. van Dorsselaer, J.-M. Lehn, Inorg. Chem. 35 (1996) 2307.
[103] P. Baxter, J.-M. Lehn, A. De Cian, J. Fischer, Angew. Chem. Int. Ed. Engl. 32 (1993) 69.
[104] P.N.W. Baxter, J.-M. Lehn, G. Baum, D. Fenske, Chem. Eur. J. 5 (1999) 102.
[105] (a) P.N.W. Baxter, J.-M. Lehn, B.O. Kneisel, G. Baum, D. Fenske, Chem. Eur. J. 5 (1999) 113;
(b) J.-M. Lehn, Supramolecular Chemistry, VCH, Weinheim, 1995, p. 155.
[106] A.M. Garcia, D.M. Bassani, J.-M. Lehn, G. Baum, D. Fenske, Chem. Eur. J. 5 (1999) 1234.
[107] B. Hasenknopf, J.-M. Lehn, N. Boumediene, A. Dupont-Gervais, A. Van Dorsellaer, B. Kneisel, D. Fenske, J. Am. Chem. Soc. 119 (1997) 10956.
[108] S. Roche, C. Haslam, H. Adams, S.L. Heath, J.A. Thomas, Chem. Commun. (1998) 1681.
[109] K.K. Klausmeyer, T.B. Rauchfuss, S.R. Wilson, Chem. Commun. (1998) 1681.
[110] B.F. Abrahams, S.J. Egan, R. Robson, J. Am. Chem. Soc. 121 (1999) 3535.
[111] B. Olenyuk, J.A. Whiteford, A. Fechtenkötter, P.J. Stang, Nature 398 (1999) 796.
[112] C.M. Drain, F. Nifiatis, A. Vasenko, J.D. Batteas, Angew. Chem. Int. Ed. Engl. 37 (1998) 2344.
[113] N. Takeda, K. Umemoto, K. Yamaguchi, M. Fujita, Nature 398 (1999) 794.
[114] B. Olenyuk, M.D. Levin, J.A. Whiteford, J.E. Shield, P.J. Stang, J. Am. Chem. Soc. 121 (1999) 10434.